We are IntechOpen,
the world's leading publisher of
Open Access books
Built by scientists, for scientists

6,900
Open access books available

185,000
International authors and editors

200M
Downloads

154
Countries delivered to

Our authors are among the

TOP 1%
most cited scientists

12.2%
Contributors from top 500 universities

BOOK CITATION INDEX
CLARIVATE ANALYTICS
INDEXED

WEB OF SCIENCE™

Selection of our books indexed in the Book Citation Index
in Web of Science™ Core Collection (BKCI)

Interested in publishing with us?
Contact book.department@intechopen.com

The Inertia Value Transformation in Maritime Applications

Holger Korte, Sven Stuppe, Jan-Hendrik Wesuls and
Tsutomu Takagi

Additional information is available at the end of the chapter

Abstract

Due to recent developments in computer technology, computer-aided investigations of structural movements in a maritime environment have become more relevant during the last years. With regard to mechanically coupled multibody systems in fishery and offshore operations, the analysis of such systems is in the focus of research and development. To analyse multibody systems, forces and moments of all included bodies have to be defined within the same reference frame, which requires a transformation algorithm. Showing the correctness of the transformation algorithm, it must be also applicable for six degrees of freedom (6DOF) motions of a free floating single body in seaways. Therefore, the computation of irregular waves is discussed before the traditional motion description of a floating structure by using the Kirchhoff equations. With these basics, an approach to calculate the motion equations of single bodies within the earth-fixed reference frame is presented before the method of the inertia value transformation. To compare the body-fixed and earth-fixed calculation method, a free-floating crew transfer vessel in irregular waves is simulated and the results are discussed. Finally, the inertia value transformation will be proved by the energy conservation principle on the example of a pure rotating rigid body with none digital calculations.

Keywords: inertia value transformation, wave-disturbed ship motions, wave-structure interaction, six degrees of freedom (6DOF), hydromechanics, inertial kinematics, Euclidian room

1. Introduction

Modern simulation techniques enable a more profound analysis of various engineering problems in an early design stage. In maritime kinematics, the focus is on the behaviour of offshore

structures under natural environment conditions like wind, waves and current. Detailed knowledge of loads and motions is required for proper dimensioning of efficient and safe systems. Furthermore, simulations are increasingly used for the design of controller-based automation and assistance systems. In addition to the accurate calculation of the structural movements, the calculation speed of a simulation is an important quality feature for these applications, e.g. real-time constraints. To determine the kinematics model of a free-floating structure in a seaway, different approaches are commonly used. The equations of motions can either be defined in the inertial reference frame or alternatively in the body-fixed reference frame. The difference between dry mechanics and maritime mechanics is based on additional hydrodynamic effects, namely, the hydrodynamic added mass, e.g. [1–3]. The hydrodynamic mass force is an inertia force. The relative acceleration between incompressible fluid and structure induces a pressure field, which results in a hydrodynamic force that is formulated as the product of the relative acceleration and a 'virtual' mass. The size of the hydrodynamic added mass depends primarily on the direction of movement and the geometry of the structure [4].

Due to the phenomenon of added or virtual masses, non-scalar and directed inertia values are necessary for describing translational and rotational motions. Probably, this results in an ordinary practice to describe floating structures within a body-fixed view, e. g. by the Kirchhoff motion equations of floating bodies [1, 3].

The investigation of mechanically coupled and multiple rigid body systems is in the focus of the authors and represents a special difficulty in this area [2, 5]. Within literature before millennium, only Paschen's algorithm was found describing dynamics of real 3D systems for fishery and mine-hunting systems with flexible, non-elastic numerical elements and rigid bodies by partially neglect of added masses [6, 7]. Later, different marine multibody systems were described with algorithms of structural mechanics [8] or as pure planar motion descriptions, e.g. [9–13]. To describe the mutual interdependencies, the equations of motions of all involved bodies have to be set up in the same coordinate system, preferably the inertial or earth-fixed system. This includes the transformation of all vectorial entities including the inertia matrices (mass matrix, moments of inertia). Therefore, the use of a transformation algorithm is required, which describes the system in the inertial reference frame. The inertia value transformation here presented, also known as Kane's method [14], was introduced by Korte and Takagi [2, 5] for fishery systems to analyse forces and motions of purse seines. Based on the principle of concentrated masses, all included nodes of the net structure are focused and connected with damped mass-spring elements. To connect the inertia values of the nodes, a transformation of the hydrodynamic added masses is required [15].

Korte et al. presented an application of the inertia value transformation for multibody systems in 2015 for a pure rotating body without elasticity [5]. The analysed scenario represents the transfer of offshore service staff from a crew transfer vessel (CTV) to a wind turbine, which is a real and environmentally affected gyro. CTV is constrained at the bow to the landing of the wind turbine in seas. The inertial reference system is located at the contact point of the structure. The ship can make an ideal rotation around all three axes of the inertial system. The motion equations of the system are defined within the inertial system to calculate the constraining forces. It was observed that temporal integration of the equations within the inertial reference frame leads to unpredictable

motions of the ship. The simulation was unstable. During development of the multibody scenario, it was discovered that an additional and oppositely directed transformation of the rotational accelerations leads to a stable solution of the simulation.

To analyse a general applicability of the inertia value transformation for maritime applications, Korte et al. defined the equations of motions for a free-floating ship with six degrees of freedom (6DOF) in the inertial reference frame [17]. Motion equations were derived from momentum and angular momentum theorem. The results of the free-floating ship were compared with ordinary simulations in the body-fixed reference frame and kinematics (see [1]).
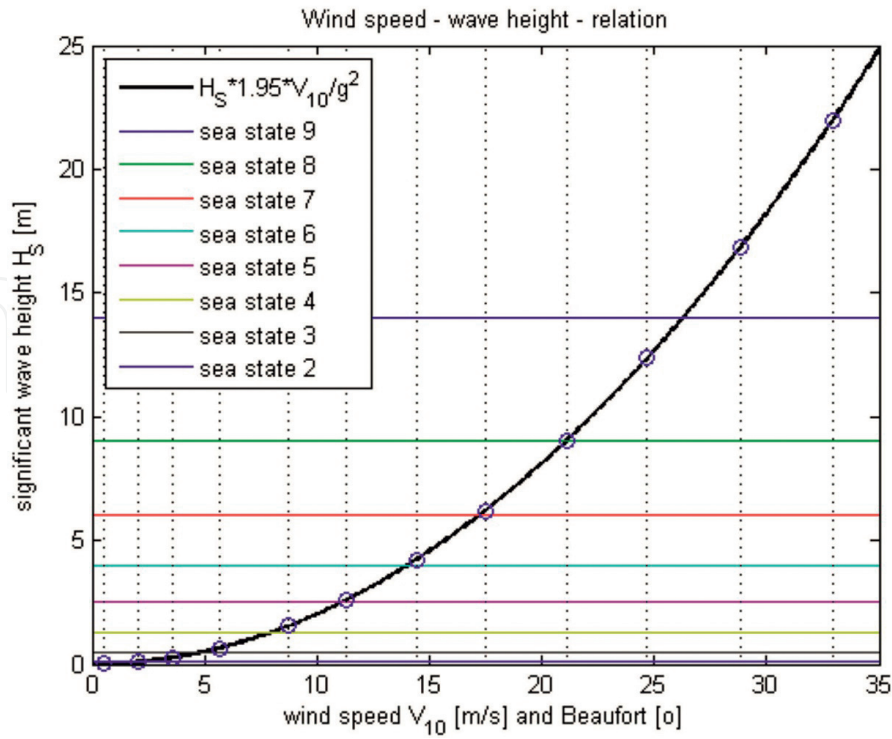
This contribution describes the applicability of the inertia value transformation in maritime applications while transferring the inertia values between a body-fixed and the inertial reference frame. The motion behaviour of the free-floating structure is in the focus of the discussion. In the following section, the modelling of the irregular seas as environmental reason of structure motions is presented. The six degrees of freedom of a floating body as well as the traditional motion equations in the body-fixed reference system are introduced afterwards. The derivation of the motion equations within the inertial reference frame by using the inertia value transformation is part of the main section. The possibility to transform the equations from inertial to body-fixed system is shown. For comparison of both methods, 6DOF simulation results of a free-floating CTV in waves are discussed. In the last section, a proof shows the energy conservation of the inertia value transformation for the case of a pure rotating rigid body.

2. Wave modelling

Depending on formation is natural irregular seas divided into wind seas and swell. Real occurred sea state phenomena are described in nautical practice as the superposition of a stochastic wind sea and two observable swells.

Wind seas are direct wind excited. The waves are rather short and steep. Due to friction, the wind transfers energy to the water surface. The resulting capillary waves with short wavelength increase the area of the free surface, whereby the effect of the energy transfer is amplified. This leads in higher and longer gravity waves, which influence the water column down to a water depth of a half wavelength. The waves propagate in the wind direction. Wind wave characteristics depend on wind speed, wind duration and fetch. The wave components of wind seas are located in the higher-frequency range of a wave spectrum. Due to containing higher frequency waves with small amplitudes, the water column oscillates inhomogeneously. Wind seas decrease by a disappearance of the wind excitation. The relation between wind classes (Beaufort wind scale) and sea-state classes (Douglas sea scale) can be seen in **Figure 1**.
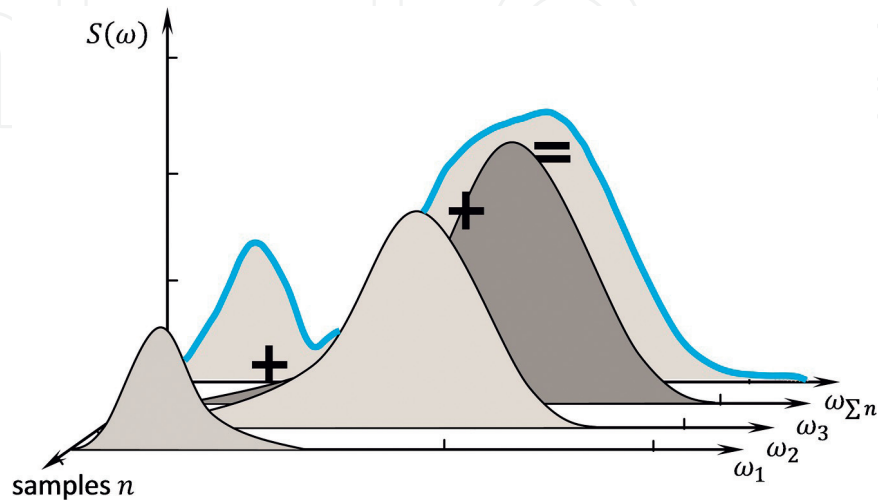
Contrary to wind seas, which is described as evolving waves, is swell the full homogeneously oscillating water column. Swell is a decaying, nearly sinusoidal wave that has moved away from the formation area, e.g. a storm region. The frequencies are in the lower range of a wave spectrum. The energy density of waves is inversely proportional to the wave frequency. Long waves with a small frequency are more energetic than short waves.

Figure 1. Relation of wind speed (Beaufort wind scale) and wave height (Douglas sea scale) for fully developed seas (modified to practice).

Irregular waves are mathematically described as superposition of a finite number of wave components with different wave frequencies, different amplitudes and different phases. The representation is carried out with energy density spectra, which have a unique distribution of the wave components for each sea area. The spectrum contains the energy $S_n(\omega)$ of all included wave frequencies. **Figure 2** shows the structure of a wave spectrum.

Relevant wave parameters can be derived from the wave spectrum. The mean wave frequency ω_0 is located at the maximum $S(\omega)$ of the spectrum. The peak period T_P is

Figure 2. Structure of a wave spectrum as superposition of different wave components.

$$T_P = \frac{2\pi}{\omega_0} \tag{1}$$

Further, wave properties can be determined with the so-called spectral moments m_n, compared with [1]. Their definition is

$$m_n = \int_0^\infty \omega^n S(\omega) d\omega \tag{2}$$

The moments up to the second order, $n = 2$, are of interest to characterise the sea state. The characteristic wave height of the spectrum is

$$H_{m0} = 4\sqrt{m_0} \tag{3}$$

and the significant wave height is

$$H_S = 3.81 \cdot \sqrt{m_0} \tag{4}$$

The period of the characteristic wave height H_{m0} is defined as

$$T_1 = \frac{m_0}{m_1} \tag{5}$$

The mean zero upcrossing period is

$$T_Z = \sqrt{\frac{m_0}{m_2}} \tag{6}$$

Variance σ^2 and standard deviation σ are

$$\sigma^2 = m_0 \tag{7}$$

$$\sigma = \sqrt{m_0} = 0.263 \cdot H_S \tag{8}$$

There are several mathematical wave spectra for computer simulations of irregular waves available, namely, the Bretschneider spectrum, the Phillips spectrum, the Pierson-Moskowitz spectrum as well as the Joint North Sea Wave Project (JONSWAP) spectrum. The most important spectra are introduced in this section.

2.1. Pierson-Moskowitz spectrum

The Pierson-Moskowitz (PM) spectrum was introduced for fully developed seas and is commonly used since 1964 [18]. It is based on long-term observation data of a weather ship in the period from 1955 to 1960. It assumes the fully developed sea, including wind sea and swell, on the North Atlantic with unlimited water depth and fetch as well as steady wind for a long time. The spectrum is

$$S_{PM}(\omega) = A \cdot \omega^{-5} \cdot e^{-B\omega^{-4}} \tag{9}$$

with parameters A and B

$$A = 0.0081 \cdot g^2 \tag{10}$$

$$B = 0.74 \left(\frac{g}{V_{wind}} \right)^4 = \frac{2.814}{H_S^2} \tag{11}$$

The relation between significant wave height and wind speed is:

$$H_S = \frac{1.95}{g^2} V_{wind}^2 \tag{12}$$

2.2. Modified Pierson-Moskowitz spectrum

After experiences with the Pierson-Moskowitz spectrum, the maritime community recommended a magnification of the spectrum [19, 20]. According to this recommendation, the parameters A and B were modified and can be determined from the observable weather parameters H_S and T_Z:

$$A = \frac{4\pi^3 H_S^2}{T_Z^4} \tag{13}$$

$$B = \frac{16\pi^3}{T_Z^4} \tag{14}$$

Figure 3 shows a comparison of the Pierson-Moskowitz spectrum and the Modified Pierson-Moskowitz (MPM) spectrum for several wind speeds. An increase of the energy density in the peak frequency of the MPM as well as a shift of the peak frequency to lower frequencies can be seen.
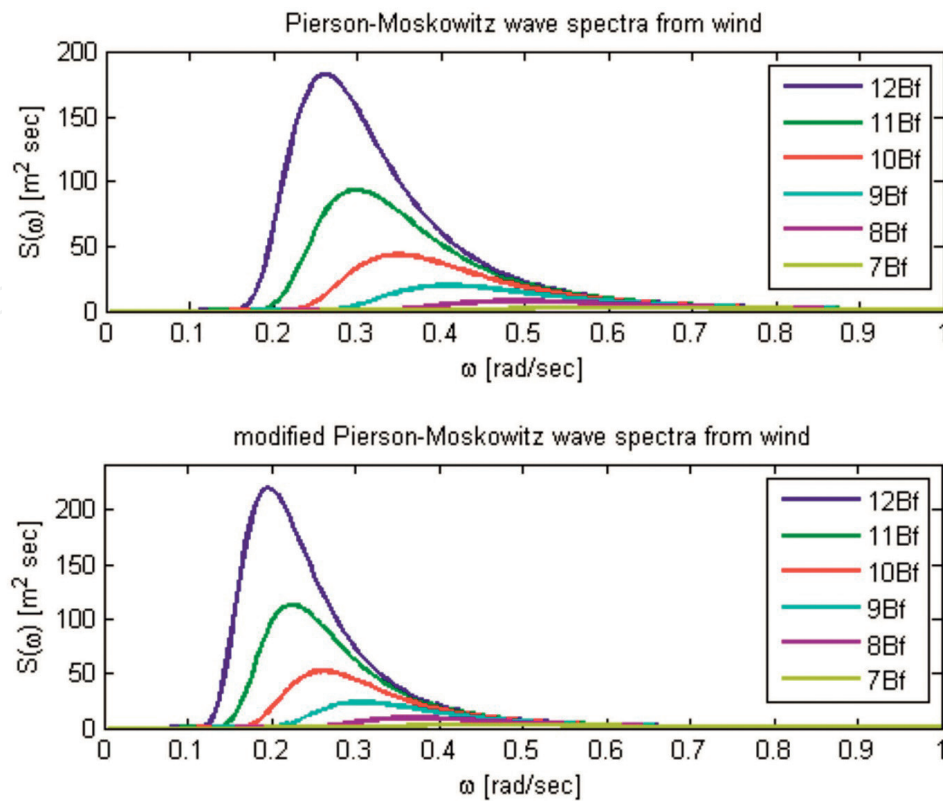
2.3. JONSWAP spectrum

The Pierson-Moskowitz spectra were developed for unlimited water depth. However, the most intensively used sea areas are often in regions of shelf seas with restrictions on the water depth and the fetch.

In 1968/1969, the characteristics of wave formations in sea areas with limited fetch and water depth were investigated exemplary for the North Sea in the international joint project 'Joint North Sea Wave Project (JONSWAP)'. During a period of approximately 10 weeks, measurements were carried out and evaluated at points reaching up to 160 km seawards in the region of the island of Sylt. The JONSWAP spectrum is based on the PM spectrum and provided with a magnification factor γ for the peak distribution.

Hasselmann's mathematical definition of the JONSWAP spectrum is [20]

$$S_{JON}(\omega) = \alpha g^2 \omega^{-5} \cdot e^{\left[-\frac{5}{4} \left(\frac{\omega_0}{\omega} \right)^4 \right]} \cdot \gamma^r \tag{15}$$

with

Figure 3. Comparison of Pierson-Moskowitz spectrum (top) and modified Pierson-Moskowitz spectrum (bottom) for several wind speeds.

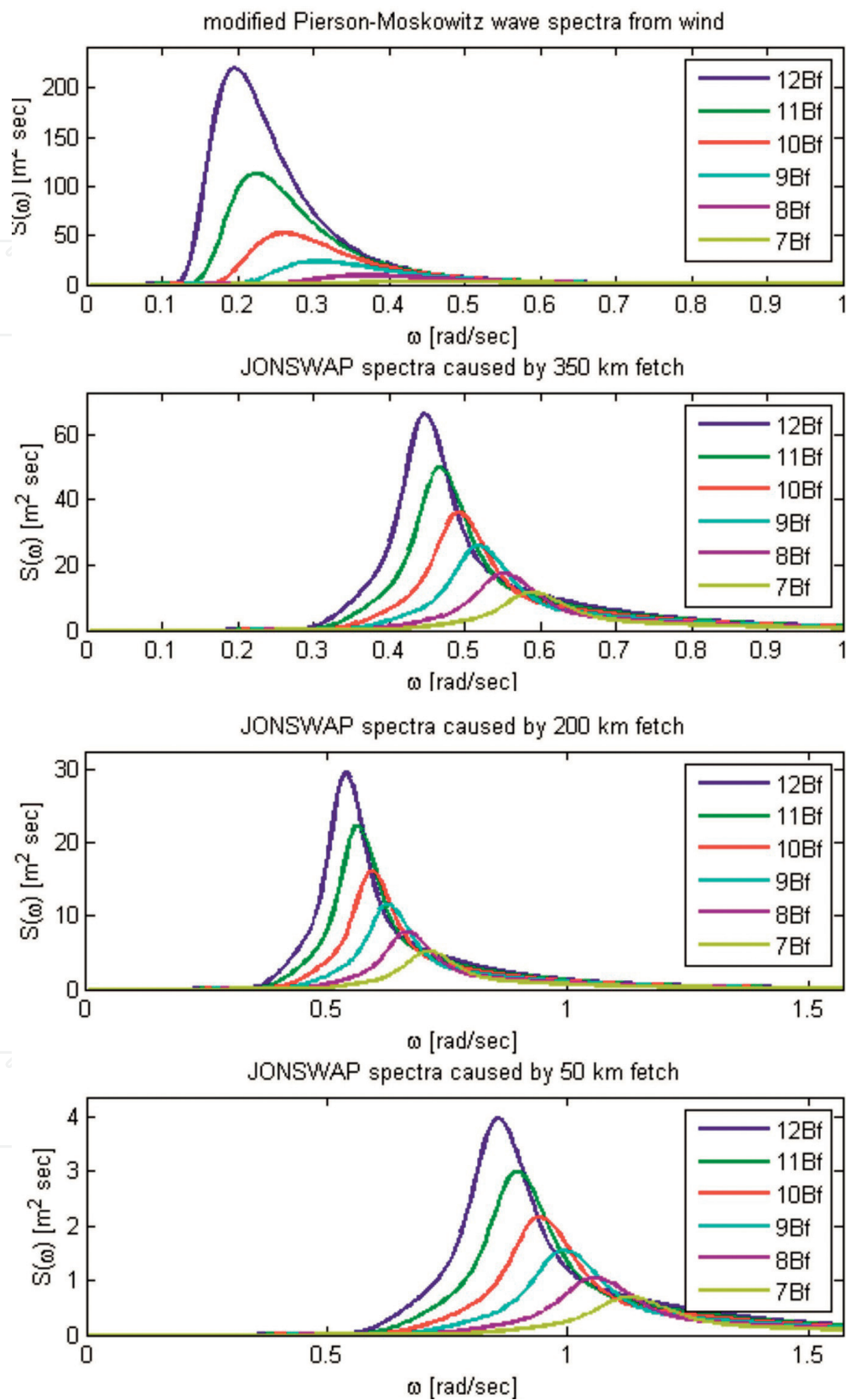$$r = e^{\left[-\frac{(\omega - \omega_0)^2}{2\sigma^2 \omega_0^2} \right]} \tag{16}$$

$$\gamma = 3.3 \tag{17}$$

$$\alpha = 0.076 \left(\frac{V_{10}^2}{F_W g} \right)^{0.22} \tag{18}$$

$$\omega_0 = 22 \left(\frac{g^2}{F_W V_{10}} \right)^{\frac{1}{3}} \tag{19}$$

$$\sigma = \begin{cases} 0.07, & \omega \leq \omega_0 \\ 0.09, & \omega > \omega_0 \end{cases} \tag{20}$$

Fetch is defined in metres and increases the wave energy linearly. A direct comparison of the JONSWAP spectrum with the MPM spectrum for a large-scale wind sea on the North Sea illustrates the lower total energy in **Figure 4**. The characteristic frequencies ω_0 of the individual wind classes are higher than those of the PM spectrum. Due to limited water depth, the wave heights are reduced. Both, the maximum of the spectrum and the area under the curve are considerable smaller than those of the reference spectrum. A comparison of seaways with different fetch lengths confirms this trend (cf. **Figure 4**). A JONSWAP spectra are used for the here presented simulations.

Figure 4. Comparison of modified Pierson-Moskowitz spectra and JONSWAP spectra for 350 km, 200 km and 50 km fetch and several wind speeds.

3. 6DOF motions of a free-floating offshore structure

In the following section, the six degrees of freedom of a ship are introduced. **Figure 5** shows a sketch of a ship hull with a body-fixed coordinate system. Body-fixed coordinate system means that the coordinate system moves with the ship. Due to advantages in determining the moments of inertia, the origin of the system is preferably located in the ships centre of gravity. The motions of a ship are described in the body-fixed coordinate system. However, the ship's position and the orientation are referenced in an earth-fixed coordinate system.
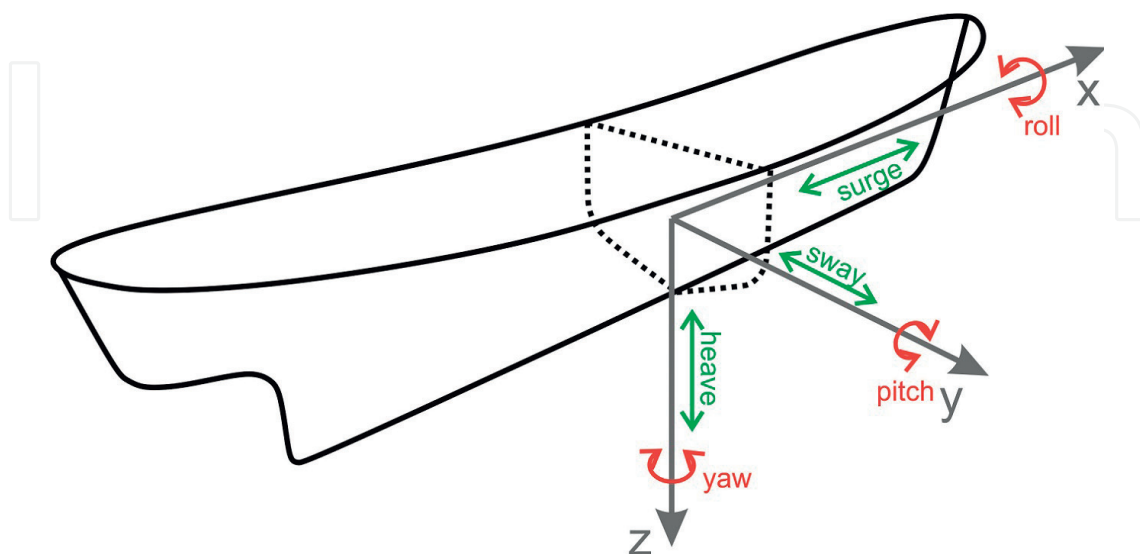
The translational motions are as follows:

- Surge: Translation along the longitudinal *x*-axis

- Sway: Translation along the transversal *y*-axis

- Heave: Translation along the vertical *z*-axis

The rotational motions are as follows:

- Roll: Rotation around the longitudinal *x*-axis

- Pitch: Rotation around the transversal *y*-axis

- Yaw: Rotation around the vertical *z*-axis

Another distinction is the classification into horizontal (surge, sway, yaw) and vertical (heave, roll, pitch) motions. The reason for this differentiation is the restoring forces caused by gravitation. These exist only for the vertical degrees of freedom. After a perturbation of the equilibrium, a ship always tends to return to it. This does not apply for horizontal motions. The result is the drift of a free-floating structure away from the original position as well as a change of the heading in case of wind, waves or current. For a driven ship or a ship in dynamic positioning mode, the ship's actuators (propeller, rudder, thruster, etc.) control the horizontal motions.

Figure 5. 6DOF motions of a free-floating ship.

4. Motion equations in the body-fixed reference system: Kirchhoff equations

As already mentioned, hydrodynamic inertial effects in the form of a hydrodynamic added mass have to be taken into account in marine applications. The mass matrix m_b (b for body) in the traditionally used body-fixed reference system is defined in Eq. (22). In the matrix, m is the physical mass and $m_{h,ij}$ is the direction-dependent content of the hydrodynamic inertia. The mass matrix is constant in the body-fixed frame. This applies analogously for the matrix of moments of inertia:

$$m_{b,ij} = m + m_{h,ij} \tag{21}$$

$$\overline{\mathbf{m}}_b = \begin{bmatrix} m + m_{h,11} & 0 & 0 \\ 0 & m + m_{h,22} & 0 \\ 0 & 0 & m + m_{h,33} \end{bmatrix} \tag{22}$$

In 1869, Kirchhoff published his work about the 'Movement of a rotating Body in a Fluid' [3]. In this work, he defined the motion equations of a floating body in a body-fixed reference system in analogy to Euler's gyro equation. The Kirchhoff equations are a system of each three equations for translation (Eq. (23)) and rotation (Eq. (24)):

$$\frac{d\vec{\mathbf{P}}}{dt} + \vec{\omega} \times \vec{\mathbf{P}} = (X, Y, Z)^{\mathsf{T}} \tag{23}$$

$$\frac{d\vec{\mathbf{L}}}{dt} + \vec{\omega} \times \vec{\mathbf{L}} + \vec{v} \times \vec{\mathbf{P}} = (K, M, N)^{\mathsf{T}} \tag{24}$$

The so-called living forces and moments depict all external forces and moments including all hydrodynamic effects, weight, buoyancy and their effect and can be found at the right-hand side of the equations inclusively. The determination of these external forces and moments is especially difficult for the horizontal degrees of freedom with a lack of restoring forces. For the simulations in this work, a simplified model is used, which considers weight, buoyancy as well as potential damping. At present, viscous effects are neglected.

The accelerations have to be integrated twice to analyse the position and orientation of the free-floating ship. The first integration is executed in the body-fixed system.

To calculate the position$(x, y, z)^{\mathsf{T}}$ and orientation$(\Phi, \Theta, \Psi)^{\mathsf{T}}$ of a floating body, the velocities have to be transformed into the inertia system. The peculiarity is the differing transformation of the rotational vector from the body-fixed system into the inertia system and vice versa, e.g. using the transformation with Euler's angles (Eq. (26), cf. [1]):

$$\vec{\omega}_e = \overline{\mathbf{C}}_{rot,be}\vec{\omega}_b \tag{25}$$

with

$$\overline{\mathbf{C}}_{rot,be} = \begin{bmatrix} 1 & s\Phi t\Theta & c\Phi t\Theta \\ 0 & c\Phi & -s\Phi \\ 0 & s\Phi/c\Theta & c\Phi/c\Theta \end{bmatrix} = \left(\overline{\mathbf{C}}_{rot,eb}\right)^{-1} \tag{26}$$

(e for earth or inertial, b for body, c for cosine, s for sine and t for tangent).

5. Motion equations in the inertial reference system

In the following section, the motion equations of a free-floating body in the earth-fixed reference system are shown. The equations are formally derived from momentum and angular momentum theorem. The transformation of the inertia values is discussed, and it is shown that a transformation of the motion equations leads to the Kirchhoff equations. It is known that the twice integration of the rotational equations results in an unstable solution. By using an additional and opposite directed transformation of the rotational accelerations, the simulations can be stabilised for longer time series.

5.1. Inertia value transformation

Kane introduced the transformation of inertia values in 1985 [14]. The used transformation matrix from the body-fixed into the earth-fixed reference system is

$$\overline{\mathbf{C}}_{be} = \begin{bmatrix} c\Theta c\Psi & s\Phi s\Theta c\Psi - c\Phi s\Psi & c\Phi s\Theta c\Psi + s\Phi s\Psi \\ c\Theta s\Psi & s\Phi s\Theta s\Psi + c\Phi c\Psi & c\Phi s\Theta s\Psi - s\Phi c\Psi \\ -s\Theta & s\Phi c\Theta & c\Phi c\Theta \end{bmatrix} \tag{27}$$

with

$$\overline{\mathbf{C}}_{be}\overline{\mathbf{C}}_{be}^{\mathsf{T}} = \begin{bmatrix} 1 & 0 & 0 \\ 0 & 1 & 0 \\ 0 & 0 & 1 \end{bmatrix} = \overline{\mathbf{C}}_{be}^{\mathsf{T}}\overline{\mathbf{C}}_{be} \tag{28}$$

and

$$\overline{\mathbf{C}}_{eb} = \overline{\mathbf{C}}_{be}^{\mathsf{T}} \tag{29}$$

The transformation of the inertia matrix is [14, 21]

$$\overline{\mathbf{J}}_e = \overline{\mathbf{C}}_{be}\overline{\mathbf{J}}_b\overline{\mathbf{C}}_{be}^{\mathsf{T}} \tag{30}$$

Analogously, it follows the transformation of the mass matrix including added mass [2]:

$$\overline{\mathbf{m}}_e = \overline{\mathbf{C}}_{be}\overline{\mathbf{m}}_b\overline{\mathbf{C}}_{be}^{\mathsf{T}} \tag{31}$$

The cross product-operator relation for matrices can be found in the literature [22, 23]:

$$\dot{\overline{\mathbf{C}}}_{be} \cdot \overline{\mathbf{C}}_{be}{}^{\mathsf{T}} = \tilde{\omega}_e = \begin{bmatrix} 0 & -\dot{\Psi} & \dot{\Theta} \\ \dot{\Psi} & 0 & -\dot{\Phi} \\ -\dot{\Theta} & \dot{\Phi} & 0 \end{bmatrix} = \left(\vec{\omega}_e \times \right) \tag{32}$$

5.2. Rotation

The rotational equations follow from angular momentum theorem, which is defined in the inertial reference frame [21, 23]:

$$\vec{L}_e = \overline{\mathbf{J}}_e \vec{\omega}_e \tag{33}$$

Taking the temporal change of the inertia matrix $\overline{\mathbf{J}}_e$ into account follows for the moment:

$$\frac{d\vec{L}_e}{dt} = \vec{\mathbf{M}}_e = \overline{\mathbf{J}}_e \dot{\vec{\omega}}_e + \dot{\overline{\mathbf{J}}}_e \vec{\omega}_e \tag{34}$$

The temporal derivative of the inertia matrix is

$$\dot{\overline{\mathbf{J}}}_e = \dot{\overline{\mathbf{C}}}_{be} \overline{\mathbf{J}}_b \overline{\mathbf{C}}_{be}{}^{\mathsf{T}} + \overline{\mathbf{C}}_{be} \overline{\mathbf{J}}_b \dot{\overline{\mathbf{C}}}_{be}{}^{\mathsf{T}} \tag{35}$$

Substituting Eq. (35) into Eq. (34) follows:

$$\vec{\mathbf{M}}_e = \overline{\mathbf{J}}_e \dot{\vec{\omega}}_e + \left(\dot{\overline{\mathbf{C}}}_{be} \overline{\mathbf{J}}_b \overline{\mathbf{C}}_{be}{}^{\mathsf{T}} + \overline{\mathbf{C}}_{be} \overline{\mathbf{J}}_b \dot{\overline{\mathbf{C}}}_{be}{}^{\mathsf{T}} \right) \vec{\omega}_e \tag{36}$$

Using the cross product-operator relation follows the momentum equation in the inertial reference system:

$$\vec{\mathbf{M}}_e = \overline{\mathbf{J}}_e \dot{\vec{\omega}}_e + \tilde{\omega}_e \overline{\mathbf{J}}_e \vec{\omega}_e = \overline{\mathbf{J}}_e \dot{\vec{\omega}}_e + \vec{\omega}_e \times \left(\overline{\mathbf{J}}_e \vec{\omega}_e \right) \tag{37}$$

The transformation of Eq. (37) into the body-fixed reference frame is

$$\vec{\mathbf{M}}_b = \overline{\mathbf{C}}_{eb} \vec{\mathbf{M}}_e = \overline{\mathbf{C}}_{eb} \overline{\mathbf{J}}_e \overline{\mathbf{C}}_{eb}{}^{\mathsf{T}} \cdot \overline{\mathbf{C}}_{eb} \dot{\vec{\omega}}_e + \overline{\mathbf{C}}_{eb} \tilde{\omega}_e \overline{\mathbf{C}}_{eb}{}^{\mathsf{T}} \cdot \overline{\mathbf{C}}_{eb} \overline{\mathbf{J}}_e \overline{\mathbf{C}}_{eb}{}^{\mathsf{T}} \cdot \overline{\mathbf{C}}_{eb} \vec{\omega}_e \tag{38}$$

It follows with

$$\vec{\mathbf{M}}_b = \overline{\mathbf{J}}_b \dot{\vec{\omega}}_b + \tilde{\omega}_b \overline{\mathbf{J}}_b \vec{\omega}_b = \overline{\mathbf{J}}_b \dot{\vec{\omega}}_b + \vec{\omega}_b \times \left(\overline{\mathbf{J}}_b \vec{\omega}_b \right) \tag{39}$$

Eq. (39) is identical to Euler's gyroscope equation, which is defined in the body-fixed system and corresponds to the Kirchhoff rotation equation (Eq. (24)) if the term $\vec{v} \times \vec{P}$ is neglected.

As already mentioned, the integration of the equations in the inertial system results in unstable behaviour. The floating body makes unpredictable, chaotic movements. It is assumed that the

instability is a consequence of the numerical inaccuracy as well as the twice integration of the equations. It was found within the project Mine Hunting 2000 that an additional and opposing transformation stabilises the simulation for longer time [6]. Due to the missing inertia value algorithm at that time, it could not be explained why. The authors assumed a numerical reason, which cannot be proved. That phenomenon of stabilisation was rebuilt for simulations of docked CTV at wind turbine tower, compare [24] with [16].

During the presented motion of the free-floating vessel, the changed rotational accelerations stabilise the system for longer periods (cf. Eq. (40)):

$$\vec{\omega}_e = \int \overline{\mathbf{C}}_{eb}\dot{\vec{\omega}}_b dt \equiv \int \overline{\mathbf{C}}_{eb}\dot{\vec{\omega}}_e dt \tag{40}$$

By using the additional transformation in the multibody application described in Ref. [16], the motions of the vessel on the wind turbine tower were stable at all times.

5.3. Translation

Consequently, the derivation of the translational equations follows the derivation of the rotational equations from the last section. The hydrodynamic added mass force is generally an external force, which defined the right-hand side of the motion equations. For the derivation of the motion equations, the hydrodynamic mass is considered as intrinsic property of the free-floating body, which has to be taken into account for every accelerated marine system. Analogously, as for the rotational inertia matrix, the mass matrix of a rotating body changes. This temporal change is equal to zero in case of pure translation.

The momentum theorem is defined in the inertial reference system:

$$\vec{P}_e = \overline{\mathbf{m}}_e \vec{v}_e \tag{41}$$

The force is the temporal derivative of the momentum:

$$\frac{d\vec{P}_e}{dt} = \vec{F}_e = \overline{\mathbf{m}}_e \dot{\vec{v}}_e + \dot{\overline{\mathbf{m}}}_e \vec{v}_e \tag{42}$$

With the transformation matrix $\overline{\mathbf{C}}_{be}$, the transformation of the mass matrix into the inertial system follows:

$$\overline{\mathbf{m}}_e = \overline{\mathbf{C}}_{be}\overline{\mathbf{m}}_b \overline{\mathbf{C}}_{be}^{\mathsf{T}} \tag{43}$$

The other direction is

$$\overline{\mathbf{m}}_b = \overline{\mathbf{C}}_{be}^{\mathsf{T}}\overline{\mathbf{m}}_e \overline{\mathbf{C}}_{be} \tag{44}$$

The temporal derivative of the mass matrix is

$$\dot{\overline{\mathbf{m}}}_e = \dot{\overline{\mathbf{C}}}_{be}\overline{\mathbf{m}}_b \overline{\mathbf{C}}_{be}^{\mathsf{T}} + \overline{\mathbf{C}}_{be}\overline{\mathbf{m}}_b \dot{\overline{\mathbf{C}}}_{be}^{\mathsf{T}} \tag{45}$$

By substituting Eq. (43) into Eq. (45) follows

$$\dot{\overline{\mathbf{m}}}_e = \dot{\overline{\mathbf{C}}}_{be}\overline{\mathbf{C}}_{be}{}^{\mathsf{T}}\overline{\mathbf{m}}_e + \overline{\mathbf{m}}_e\overline{\mathbf{C}}_{be}\dot{\overline{\mathbf{C}}}_{be}{}^{\mathsf{T}} \tag{46}$$

and by using the cross product-operator relation

$$\dot{\overline{\mathbf{m}}}_e = \tilde{\omega}_e\overline{\mathbf{m}}_e + \overline{\mathbf{m}}_e\left(-\tilde{\omega}_e\right) \tag{47}$$

Substituting Eq. (47) into Eq. (42) results in the translational equation for a floating body in the inertial reference frame:

$$\vec{F}_e = \overline{\mathbf{m}}_e\dot{\vec{v}}_e + \tilde{\omega}_e\left(\overline{\mathbf{m}}_e\vec{v}_e\right) - \left(\overline{\mathbf{m}}_e\tilde{\omega}_e\right)\vec{v}_e = \overline{\mathbf{m}}_e\dot{\vec{v}}_e + \vec{\omega}_e \times \left(\overline{\mathbf{m}}_e\vec{v}_e\right) - \overline{\mathbf{m}}_e\vec{\omega}_e \times \vec{v}_e \tag{48}$$

Eq. (48) contains only values of the inertial reference system. Due to change of the orientation and the non-scalar characteristic of the mass matrix, Eq. (48) contains two additional terms. These terms disappear for each application where the hydrodynamic added mass is not considered and the mass is scalar, e.g. in aerospace industries or robotics. In case of pure translation, these terms are equal to zero too, and the equation results in Newton's second law.

In the following equation, the transformation of Eq. (48) into the body-fixed reference system is shown. The relation of the velocity in both systems is

$$\vec{v}_e = \overline{\mathbf{C}}_{be}\vec{v}_b \tag{49}$$

In case of simultaneous rotation and translation, the rotation matrix changes. The acceleration in inertial frame is

$$\dot{\vec{v}}_e = \dot{\overline{\mathbf{C}}}_{be}\vec{v}_b + \overline{\mathbf{C}}_{be}\dot{\vec{v}}_b \tag{50}$$

(Remark: In case of pure translation, $\dot{\vec{v}}_e = \mathbf{C}_{be}\dot{\vec{v}}_b$).

By inserting identity matrix, Eq. (28) follows:

$$\dot{\vec{v}}_e = \dot{\overline{\mathbf{C}}}_{be}\overline{\mathbf{C}}_{be}{}^{\mathsf{T}}\overline{\mathbf{C}}_{be}\vec{v}_b + \overline{\mathbf{C}}_{be}\dot{\vec{v}}_b \tag{51}$$

This is identical to

$$\dot{\vec{v}}_e = \tilde{\omega}_e\vec{v}_e + \overline{\mathbf{C}}_{be}\dot{\vec{v}}_b = \vec{\omega}_e \times \vec{v}_e + \overline{\mathbf{C}}_{be}\dot{\vec{v}}_b \tag{52}$$

Substituting Eq. (52) into Eq. (48), the term $\left(\overline{\mathbf{m}}_e\tilde{\omega}_e\right)\vec{v}_e$ disappears, and Eq. (48) becomes

$$\vec{F}_e = \overline{\mathbf{m}}_e\overline{\mathbf{C}}_{be}\dot{\vec{v}}_b + \tilde{\omega}_e\left(\overline{\mathbf{m}}_e\vec{v}_e\right) \tag{53}$$

The transformation of Eq. (53) into the body-fixed reference frame is

$$\vec{F}_b = \overline{\mathbf{C}}_{eb}\vec{F}_e = \overline{\mathbf{C}}_{eb}\overline{\mathbf{m}}_e\overline{\mathbf{C}}_{eb}^{\mathsf{T}}\cdot\overline{\mathbf{C}}_{eb}\overline{\mathbf{C}}_{be}\dot{\vec{v}}_b + \overline{\mathbf{C}}_{eb}\tilde{\boldsymbol{\omega}}_e\overline{\mathbf{C}}_{eb}^{\mathsf{T}}\cdot\overline{\mathbf{C}}_{eb}\overline{\mathbf{m}}_e\overline{\mathbf{C}}_{eb}^{\mathsf{T}}\overline{\mathbf{C}}_{eb}\vec{v}_e \tag{54}$$

Replacing the values from inertial system with values from body-fixed system follows:

$$\vec{F}_b = \overline{\mathbf{m}}_b\dot{\vec{v}}_b + \tilde{\boldsymbol{\omega}}_b\overline{\mathbf{m}}_b\vec{v}_b = \overline{\mathbf{m}}_b\dot{\vec{v}}_b + \vec{\boldsymbol{\omega}}_b \times \left(\overline{\mathbf{m}}_b\vec{v}_b\right) \tag{55}$$

Eq. (55) corresponds to the translational Kirchhoff equation (Eq. (23)) in the body-fixed system.

6. Simulations in body-fixed and inertial reference frame

The following section shows simulation comparisons of a free-floating vessel in both reference systems. 6DOF motion simulations are performed for various wave conditions. The hydrodynamic model of the simulation is implemented in MATLAB/Simulink.

6.1. Parameterisation of the ship

The simulated ship is a crew transfer vessel, which is used for the transfer of offshore service staff in the German Bight. **Figure 6** shows a snapshot of the ship's CAD model. It is a catamaran hull with a length of $L_{oA} = 22.0\ m$, a breadth of $B = 8.3\ m$ and a mass of $m = 60\ t$. For the simulation, the hydrodynamic parameters like hydrodynamic added masses and moments of inertia, as well as the potential damping coefficients of the CTV, are required. They were determined within the project 'Safe Offshore Operations (SOOP)' using the potential radiation and diffraction programme WAMIT (cf. [24]). The ship is discretised station-wise

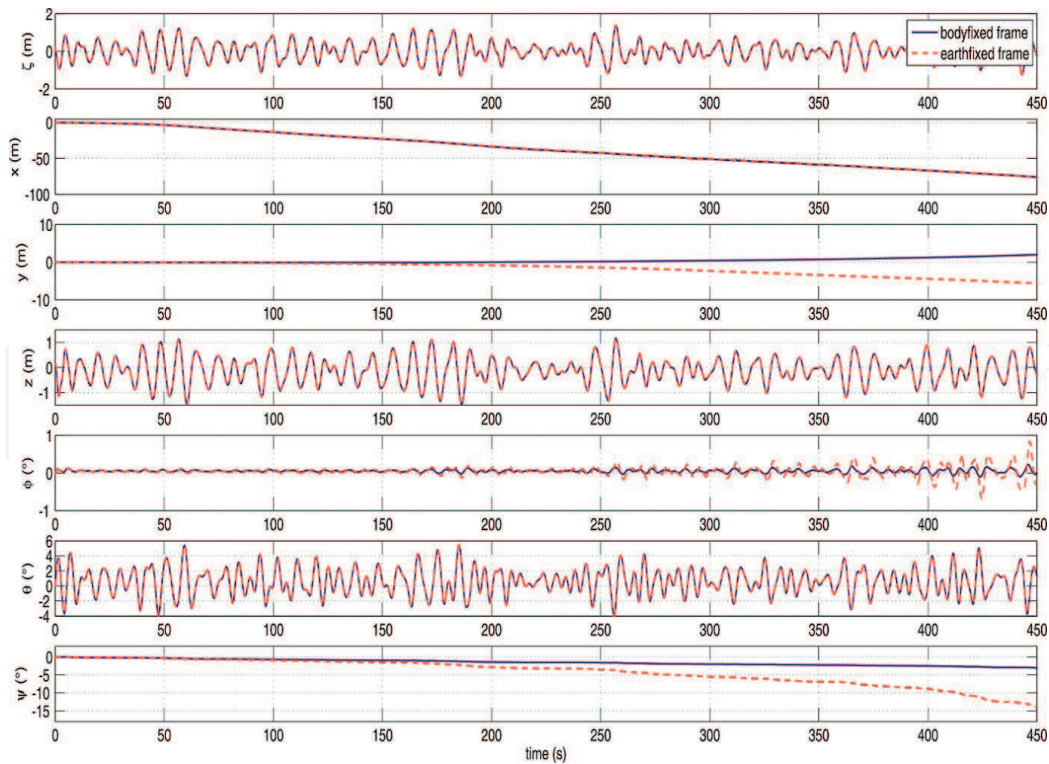**Figure 6.** CAD snapshot of the simulated crew transfer vessel.

to calculate wave-induced forces and moments. The calculated forces are buoyancy and weight as well as potential damping force.
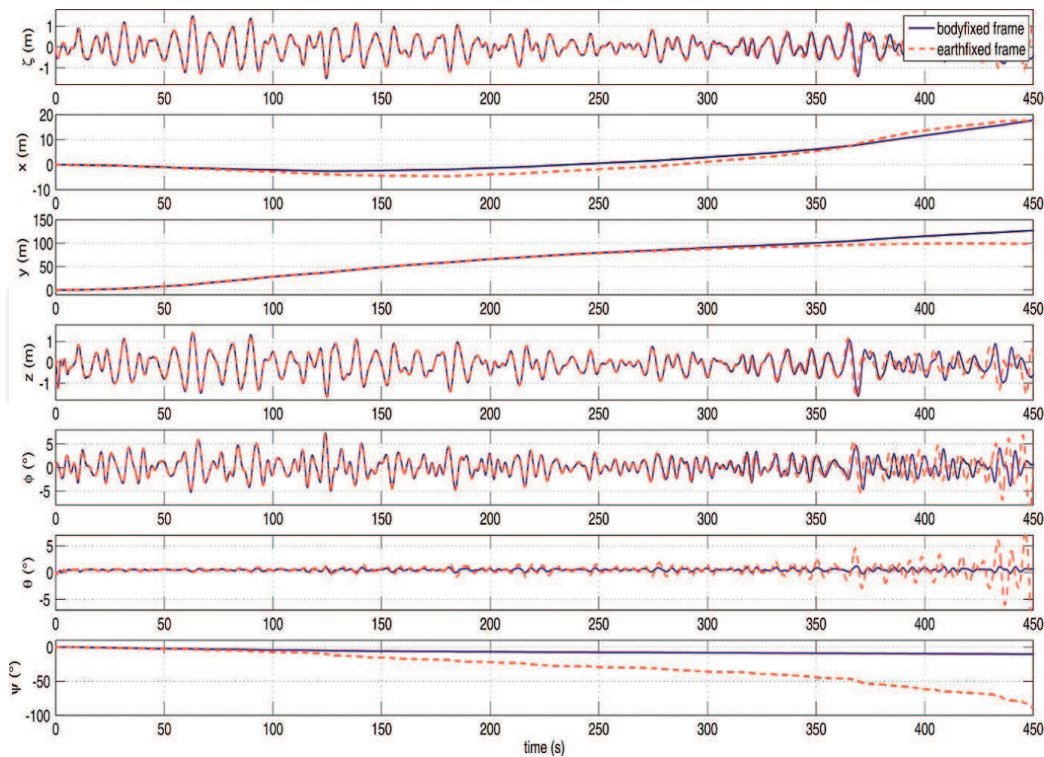
6.2. 6DOF simulations

The following figures show the comparison of the CTV 6DOF body motions in irregular seas. The ship is free floating with no initial velocity. **Figure 7** shows the simulation results for the case of head seas and **Figure 8** for beam seas. The wind wave parameters are a significant wave height of $H_S = 2.1\ m$ and a peak period of $\omega_0 = 0.7\ rad/s$. Swell is neglected.

The figures show from top to bottom the registered wave elevation at the ships centre of gravity, the x-, y- and z-position as well as the orientation angles Φ, Θ and Ψ. Blue curves are for the body-fixed reference frame and red curves for simulations in the inertial reference frame.

At the beginning of the presented simulations, the motion behaviour in both reference systems shows an identical behaviour. In further process, however, an increasing deviation of the ship's heading in the inertial reference is registered. The result is a changing encounter angle of ship and waves. For the case of head seas, the ship begins to move in transverse direction and to roll. In the beam seas, simulation leads the changed encounter angle in a pitch motion. In total, it can be seen that the comparison of vertical motions shows an identical behaviour. As already mentioned, the yaw motion is controlled in case of a driven ship. It is assumed that the motions in both reference systems are identical in this case. Analysis of yaw motion is the subject of the present work. It has to be pointed out that the simulations in the inertial reference system were

Figure 7. Comparison of the ship position and orientation for head seas. Solid line for body-fixed reference frame. Dashed line for inertial reference frame.

Figure 8. Comparison of the ship position and orientation for beam seas. Solid line for body-fixed reference frame. Dashed line for inertial reference frame.

unstable after longer simulation time. Instability occurs abruptly. Intensive analysis of the instability reason is also the subject of the present work.

7. Proof of energy conservation for rotatory inertia value transformation

Problem: Common practice in calculating rotational motions of rigid bodies applies the so-called *angular velocity transformation* between a first integration over time in body-fixed frame and a second within inertial frame (see [1]). This is contrary to the so-called *linear velocity transformation*, which uses the ordinary vector transformation algorithm as applied in our solution [2], e.g. Euler's angle transformation. The derivation of the rotation matrix $\overline{\mathbf{C}}_{rot,be}$ (Eq. (26)) is carried out by observations and describes the rotation around the three body-fixed coordinate axes sequentially in time.

In 1995, Blass and Gurevich postulates 'Matrix Transformation Is Complete for the Average Case' [25]:

$$\overline{A}_e = \overline{\mathbf{C}}_b^e \cdot \overline{A}_b \cdot \left(\overline{\mathbf{C}}_b^e\right)^{-1} \tag{56}$$

whereby $\overline{\mathbf{C}}_b^e$ describes the ordinary transformation matrix for vector values from coordinate system b, here body fixed, to the inertial or earth-fixed ones e. Which transformation is correct, way I in comparison to Eq. (25) or way II regarding Eqs. (30) and (49)?

I: if $\vec{\omega}_e = \overline{\mathbf{C}}_{rot,be} \cdot \vec{\omega}_b$ is true; also,

$\vec{\mathbf{M}}_e = \overline{\mathbf{C}}_{rot,be} \cdot \overline{\mathbf{J}}_b \cdot \left(\overline{\mathbf{C}}_{rot,be}\right)^{-1} \cdot \overline{\mathbf{C}}_{rot,be} \cdot \vec{\omega}_b$ might be possible being true, but wrong in our opinion, because $\left|\overline{\mathbf{C}}_{rot,be}\right| \neq 1$ for each $\Theta \neq 0$

or II: if $\vec{\omega}_e = \overline{\mathbf{C}}_b^e \cdot \vec{\omega}_b$ is true, contrary to the above

$\vec{\mathbf{M}}_e = \overline{\mathbf{C}}_b^e \cdot \overline{\mathbf{J}}_b \cdot \left(\overline{\mathbf{C}}_b^e\right)^{\mathsf{T}} \cdot \overline{\mathbf{C}}_b^e \cdot \vec{\omega}_b$ have to be true!

Matrix mathematics cannot give answer, because both assumptions are valid.

Authors expect calculus II as valid due to the correct transformation of the moment vector.

Its correctness may prove only by the general use of one physical principal of conservation. For that purpose, the energy conservation shall be applied. Therefore, the pure rotating energy from one mass point of the rigid body (see *step 1*) has to be compared with the kinetic energy of same mass point and motion applying continuum physics within FEM methods (see *step 2*). Furthermore and in accordance with authors who claim of wrong description of rotatory kinetic energy within the body-fixed frame, all used rotation speed components are time derivatives of inertial-fixed Euler's angles. Within the calculation of *step 3*, it has to be shown that all coefficients of both energy equations are equal, otherwise the proof fails.

7.1. Calculation of rotatory kinetic energy of a mass point from a rotating body (*step 1*)

Vector value transformation based on Eulerian angles $\vec{\mathbf{\Pi}}_e = \left(\Phi \ \ \Theta \ \ \Psi\right)^{\mathsf{T}}$ using the well known transformation matrix, compare with [1] (Eq. (27)). The components C_{ij} of rotation matrix are

$$\overline{\mathbf{C}}_b^e = \begin{bmatrix} C_{11} & C_{12} & C_{13} \\ C_{21} & C_{22} & C_{23} \\ C_{31} & C_{32} & C_{33} \end{bmatrix} = \begin{bmatrix} c\Theta c\Psi & s\Phi s\Theta c\Psi - c\Phi s\Psi & c\Phi s\Theta c\Psi + s\Phi s\Psi \\ c\Theta s\Psi & s\Phi s\Theta s\Psi + c\Phi c\Psi & c\Phi s\Theta s\Psi - s\Phi c\Psi \\ -s\Theta & s\Phi c\Theta & c\Phi c\Theta \end{bmatrix} \tag{57}$$

The rotatory inertia value $\overline{\mathbf{J}}_{dm}$ of the mass point calculates

$$\overline{\mathbf{J}}_{dm} \cdot dm = dm \cdot \begin{bmatrix} R_y^2 + R_z^2 & -R_x R_y & -R_x R_z \\ -R_x R_y & R_x^2 + R_z^2 & -R_y R_z \\ -R_x R_z & -R_y R_z & R_x^2 + R_y^2 \end{bmatrix} \tag{58}$$

by angular speed

$$\dot{\vec{\mathbf{\Pi}}}_e = \vec{\omega}_e = \left(\dot{\Phi} \ \ \dot{\Theta} \ \ \dot{\Psi}\right)^{\mathsf{T}} \tag{59}$$

and lever arm $\vec{\mathbf{R}}_m = \left(R_x \ \ R_y \ \ R_z\right)^{\mathsf{T}}$ from the bodies' centre of gravity to the mass point in body-fixed frame *b*. By vectorial depiction, the rotatory kinetic energy can be formulated as follows, e.g. Ginsberg [21]:

$$E_{rot} = \frac{1}{2} dm \cdot \vec{\omega}_e^{\mathrm{T}} \cdot \left(\overline{\mathbf{C}}_b^e \cdot \overline{\mathbf{J}}_{dm} \cdot \overline{\mathbf{C}}_e^b \right) \cdot \vec{\omega}_e \tag{60}$$

The first calculation step can be $\overline{\mathbf{C}}_e^b \cdot \vec{\omega}_e$ (cf. Eq. (61)):

$$\overline{\mathbf{C}}_e^b \cdot \vec{\omega}_e = \begin{bmatrix} C_{11}\dot{\Phi} + C_{21}\dot{\Theta} + C_{31}\dot{\Psi} \\ C_{12}\dot{\Phi} + C_{22}\dot{\Theta} + C_{32}\dot{\Psi} \\ C_{13}\dot{\Phi} + C_{23}\dot{\Theta} + C_{33}\dot{\Psi} \end{bmatrix} \tag{61}$$

Now, $\overline{\mathbf{J}}_{dm} \cdot \overline{\mathbf{C}}_e^b \cdot \vec{\omega}_e$ can be estimated:

$$\begin{bmatrix} R_y^2 + R_z^2 & -R_x R_y & -R_x R_z \\ -R_x R_y & R_x^2 + R_z^2 & -R_y R_z \\ -R_x R_z & -R_y R_z & R_x^2 + R_y^2 \end{bmatrix} \cdot \begin{bmatrix} C_{11}\dot{\Phi} + C_{21}\dot{\Theta} + C_{31}\dot{\Psi} \\ C_{12}\dot{\Phi} + C_{22}\dot{\Theta} + C_{32}\dot{\Psi} \\ C_{13}\dot{\Phi} + C_{23}\dot{\Theta} + C_{33}\dot{\Psi} \end{bmatrix} =$$

$$\begin{bmatrix} C_{11}R_y^2\dot{\Phi} + C_{11}R_z^2\dot{\Phi} + C_{21}R_y^2\dot{\Theta} + C_{21}R_z^2\dot{\Theta} + C_{31}R_y^2\dot{\Psi} + C_{31}R_z^2\dot{\Psi} \ldots \\ -C_{12}R_x R_y\dot{\Phi} - C_{22}R_x R_y\dot{\Theta} - C_{32}R_x R_y\dot{\Psi} - C_{13}R_x R_z\dot{\Phi} - C_{23}R_x R_z\dot{\Theta} - C_{33}R_x R_z\dot{\Psi} \\ -C_{11}R_x R_y\dot{\Phi} - C_{21}R_x R_y\dot{\Theta} - C_{31}R_x R_y\dot{\Psi} + C_{12}R_x^2\dot{\Phi} + C_{12}R_z^2\dot{\Phi} + C_{22}R_x^2\dot{\Theta} \ldots \\ +C_{22}R_z^2\dot{\Theta} + C_{32}R_x^2\dot{\Psi} + C_{32}R_z^2\dot{\Psi} - C_{13}R_y R_z\dot{\Phi} - C_{23}R_y R_z\dot{\Theta} - C_{33}R_y R_z\dot{\Psi} \\ -C_{11}R_x R_z\dot{\Phi} - C_{21}R_x R_z\dot{\Theta} - C_{31}R_x R_z\dot{\Psi} - C_{12}R_y R_z\dot{\Phi} - C_{22}R_y R_z\dot{\Theta} - C_{32}R_y R_z\dot{\Psi} \ldots \\ C_{13}R_x^2\dot{\Phi} + C_{13}R_y^2\dot{\Phi} + C_{23}R_x^2\dot{\Theta} + C_{23}R_y^2\dot{\Theta} + C_{33}R_x^2\dot{\Psi} + C_{33}R_y^2\dot{\Psi} \end{bmatrix} \tag{62}$$

In the following equation, the transposed vector from Eq. (61) is multiplied with the vector of Eq. (62):

$$\left(\overline{\mathbf{C}}_e^b \cdot \vec{\omega}_e \right)^{\mathrm{T}} \cdot \overline{\mathbf{J}}_{dm} \cdot \overline{\mathbf{C}}_e^b \cdot \vec{\omega}_e = E_1 + E_2 + E_3 \tag{63}$$

getting three components of a sum E_1 to E_3:

$$E_1 = C_{11}^2 R_y^2 \dot{\Phi}^2 + C_{11}^2 R_z^2 \dot{\Phi}^2 + C_{11}C_{21}R_y^2\dot{\Phi}\dot{\Theta} + C_{11}C_{21}R_z^2\dot{\Phi}\dot{\Theta} + C_{11}C_{31}R_y^2\dot{\Phi}\dot{\Psi} \ldots$$

$$+ C_{11}C_{31}R_z^2\dot{\Phi}\dot{\Psi} - C_{11}C_{12}R_x R_y\dot{\Phi}^2 - C_{11}C_{22}R_x R_y\dot{\Phi}\dot{\Theta} - C_{11}C_{32}R_x R_y\dot{\Phi}\dot{\Psi} \ldots$$

$$- C_{11}C_{13}R_x R_z\dot{\Phi}^2 - C_{11}C_{23}R_x R_z\dot{\Phi}\dot{\Theta} - C_{11}C_{33}R_x R_z\dot{\Phi}\dot{\Psi} + C_{11}C_{21}R_y^2\dot{\Phi}\dot{\Theta} + C_{21}^2 R_z^2\dot{\Theta}^2 \ldots$$

$$+ C_{11}C_{21}R_z^2\dot{\Phi}\dot{\Theta} + C_{21}^2 R_y^2\dot{\Theta}^2 + C_{21}C_{31}R_y^2\dot{\Theta}\dot{\Psi} + C_{21}C_{31}R_z^2\dot{\Theta}\dot{\Psi} - C_{12}C_{21}R_x R_y\dot{\Phi}\dot{\Theta} \ldots$$

$$- C_{21}C_{22}R_x R_y\dot{\Theta}^2 - C_{21}C_{32}R_x R_y\dot{\Theta}\dot{\Psi} - C_{13}C_{21}R_x R_z\dot{\Phi}\dot{\Theta} - C_{21}C_{23}R_x R_z\dot{\Theta}^2 \ldots$$

$$- C_{21}C_{33}R_x R_z\dot{\Theta}\dot{\Psi} + C_{11}C_{31}R_y^2\dot{\Phi}\dot{\Psi} + C_{11}C_{31}R_z^2\dot{\Phi}\dot{\Psi} + C_{21}C_{31}R_y^2\dot{\Theta}\dot{\Psi} + C_{21}C_{31}R_z^2\dot{\Theta}\dot{\Psi} \ldots$$

$$+ C_{31}^2 R_y^2\dot{\Psi}^2 + C_{31}^2 R_z^2\dot{\Psi}^2 - C_{12}C_{31}R_x R_y\dot{\Phi}\dot{\Psi} - C_{22}C_{31}R_x R_y\dot{\Theta}\dot{\Psi} - C_{32}C_{31}R_x R_y\dot{\Psi}^2 \ldots$$

$$- C_{13}C_{31}R_x R_z\dot{\Phi}\dot{\Psi} - C_{23}C_{31}R_x R_z\dot{\Theta}\dot{\Psi} - C_{31}C_{33}R_x R_z\dot{\Psi}^2$$

$$\begin{aligned}
E_2 =\; & -C_{11}C_{12}R_xR_y\dot{\Phi}^2 - C_{12}C_{21}R_xR_y\dot{\Phi}\dot{\Theta} - C_{12}C_{31}R_xR_y\dot{\Phi}\dot{\Psi} + C_{12}^2R_x^2\dot{\Phi}^2 + C_{12}^2R_z^2\dot{\Phi}^2\ldots \\
& + C_{12}C_{22}R_x^2\dot{\Phi}\dot{\Theta} + C_{12}C_{22}R_z^2\dot{\Phi}\dot{\Theta} + C_{12}C_{32}R_x^2\dot{\Phi}\dot{\Psi} + C_{12}C_{32}R_z^2\dot{\Phi}\dot{\Psi} - C_{12}C_{13}R_yR_z\dot{\Phi}^2\ldots \\
& - C_{12}C_{23}R_yR_z\dot{\Phi}\dot{\Theta} - C_{12}C_{33}R_yR_z\dot{\Phi}\dot{\Psi} - C_{11}C_{22}R_xR_y\dot{\Phi}\dot{\Theta} - C_{21}C_{22}R_xR_y\dot{\Theta}^2\ldots \\
& - C_{22}C_{31}R_xR_y\dot{\Theta}\dot{\Psi} + C_{12}C_{22}R_x^2\dot{\Phi}\dot{\Theta} + C_{12}C_{22}R_z^2\dot{\Phi}\dot{\Theta} + C_{22}^2R_x^2\dot{\Theta}^2 + C_{22}^2R_z^2\dot{\Theta}^2\ldots \\
& + C_{22}C_{32}R_x^2\dot{\Theta}\dot{\Psi} + C_{22}C_{32}R_z^2\dot{\Theta}\dot{\Psi} - C_{13}C_{22}R_yR_z\dot{\Phi}\dot{\Theta} - C_{22}C_{23}R_yR_z\dot{\Theta}^2\ldots \\
& - C_{22}C_{33}R_yR_z\dot{\Theta}\dot{\Psi} - C_{11}C_{32}R_xR_y\dot{\Phi}\dot{\Psi} - C_{21}C_{32}R_xR_y\dot{\Theta}\dot{\Psi} - C_{31}C_{32}R_xR_y\dot{\Psi}^2\ldots \\
& + C_{12}C_{32}R_x^2\dot{\Phi}\dot{\Psi} + C_{12}C_{32}R_z^2\dot{\Phi}\dot{\Psi} + C_{22}C_{32}R_x^2\dot{\Theta}\dot{\Psi} + C_{22}C_{32}R_z^2\dot{\Theta}\dot{\Psi} + C_{32}^2R_x^2\dot{\Psi}^2\ldots \\
& + C_{32}^2R_z^2\dot{\Psi}^2 - C_{13}C_{32}R_yR_z\dot{\Phi}\dot{\Psi} - C_{23}C_{32}R_yR_z\dot{\Theta}\dot{\Psi} - C_{32}C_{33}R_yR_z\dot{\Psi}^2
\end{aligned}$$

$$\begin{aligned}
E_3 =\; & -C_{11}C_{13}R_xR_z\dot{\Phi}^2 - C_{13}C_{21}R_xR_z\dot{\Phi}\dot{\Theta} - C_{13}C_{31}R_xR_z\dot{\Phi}\dot{\Psi} - C_{12}C_{13}R_yR_z\dot{\Phi}^2\ldots \\
& - C_{13}C_{22}R_yR_z\dot{\Phi}\dot{\Theta} - C_{13}C_{32}R_yR_z\dot{\Phi}\dot{\Psi} + C_{13}^2R_x^2\dot{\Phi}^2 + C_{13}^2R_y^2\dot{\Phi}^2 + C_{13}C_{23}R_x^2\dot{\Phi}\dot{\Theta}\ldots \\
& + C_{13}C_{23}R_y^2\dot{\Phi}\dot{\Theta} + C_{13}C_{33}R_x^2\dot{\Phi}\dot{\Psi} + C_{13}C_{33}R_y^2\dot{\Phi}\dot{\Psi} - C_{11}C_{23}R_xR_z\dot{\Phi}\dot{\Theta}\ldots \\
& - C_{21}C_{23}R_xR_z\dot{\Theta}^2 - C_{23}C_{31}R_xR_z\dot{\Theta}\dot{\Psi} - C_{12}C_{23}R_yR_z\dot{\Phi}\dot{\Theta} - C_{22}C_{23}R_yR_z\dot{\Theta}^2\ldots \\
& - C_{23}C_{32}R_yR_z\dot{\Theta}\dot{\Psi} + C_{13}C_{23}R_x^2\dot{\Phi}\dot{\Theta} + C_{13}C_{23}R_y^2\dot{\Phi}\dot{\Theta} + C_{23}^2R_x^2\dot{\Theta}^2 + C_{23}^2R_y^2\dot{\Theta}^2\ldots \\
& + C_{23}C_{33}R_x^2\dot{\Theta}\dot{\Psi} + C_{23}C_{33}R_y^2\dot{\Theta}\dot{\Psi} - C_{11}C_{33}R_xR_z\dot{\Phi}\dot{\Psi} - C_{21}C_{33}R_xR_z\dot{\Theta}\dot{\Psi}\ldots \\
& - C_{31}C_{33}R_xR_z\dot{\Psi}^2 - C_{12}C_{33}R_yR_z\dot{\Phi}\dot{\Psi} - C_{22}C_{33}R_yR_z\dot{\Theta}\dot{\Psi} - C_{32}C_{33}R_yR_z\dot{\Psi}^2\ldots \\
& + C_{13}C_{33}R_x^2\dot{\Phi}\dot{\Psi} + C_{13}C_{33}R_y^2\dot{\Phi}\dot{\Psi} + C_{23}C_{33}R_x^2\dot{\Theta}\dot{\Psi} + C_{23}C_{33}R_y^2\dot{\Theta}\dot{\Psi} + C_{33}^2R_x^2\dot{\Psi}^2\ldots \\
& + C_{33}^2R_y^2\dot{\Psi}^2
\end{aligned}$$

Finally, the sum of these components E_1, E_2 and E_3 has to be multiplied by the factor ½ dm to get the rotatory kinetic energy. Because that factor is implemented also within the second energy equation (*step 2*), the energy components can be summarised and compared directly with Eq. (68). By sorting all components to the lever arm and rotating speed combinations, we get Eq. (64):

$$\begin{aligned}
\frac{2E_{rot}}{dm} =\; & \left(C_{32}^2 + C_{33}^2\right)R_x^2\dot{\Psi}^2 - 2C_{31}C_{32}R_xR_y\dot{\Psi}^2 - 2C_{31}C_{33}R_xR_z\dot{\Psi}^2 - 2C_{32}C_{33}R_yR_z\dot{\Psi}^2\ldots \\
& + \left(C_{31}^2 + C_{33}^2\right)R_y^2\dot{\Psi}^2 + \left(C_{31}^2 + C_{32}^2\right)R_z^2\dot{\Psi}^2 + 2(C_{22}C_{32} + C_{23}C_{33})R_x^2\dot{\Theta}\dot{\Psi}\ldots \\
& - 2(C_{22}C_{31} + C_{21}C_{32})R_xR_y\dot{\Theta}\dot{\Psi} - 2(C_{21}C_{33} + C_{23}C_{31})R_xR_z\dot{\Theta}\dot{\Psi}\ldots \\
& - 2(C_{22}C_{33} + C_{23}C_{32})R_yR_z\dot{\Theta}\dot{\Psi} + 2(C_{23}C_{33} + C_{21}C_{31})R_y^2\dot{\Theta}\dot{\Psi}\ldots \\
& + 2(C_{22}C_{32} + C_{21}C_{31})R_z^2\dot{\Theta}\dot{\Psi} + 2(C_{13}C_{33} + C_{12}C_{32})R_x^2\dot{\Phi}\dot{\Psi}\ldots \\
& - 2(C_{12}C_{31} + C_{11}C_{32})R_xR_y\dot{\Phi}\dot{\Psi} - 2(C_{11}C_{33} + C_{13}C_{31})R_xR_z\dot{\Phi}\dot{\Psi}\ldots \\
& - 2(C_{12}C_{33} + C_{13}C_{32})R_yR_z\dot{\Phi}\dot{\Psi} + 2(C_{13}C_{33} + C_{11}C_{31})R_y^2\dot{\Phi}\dot{\Psi}\ldots \\
& + 2(C_{12}C_{32} + C_{11}C_{31})R_z^2\dot{\Phi}\dot{\Psi} + \left(C_{22}^2 + C_{23}^2\right)R_x^2\dot{\Theta}^2 - 2C_{21}C_{22}R_xR_y\dot{\Theta}^2\ldots \\
& - 2C_{21}C_{23}R_xR_z\dot{\Theta}^2 - 2C_{22}C_{23}R_yR_z\dot{\Theta}^2 + \left(C_{21}^2 + C_{23}^2\right)R_y^2\dot{\Theta}^2 + \left(C_{21}^2 + C_{22}^2\right)R_z^2\dot{\Theta}^2\ldots \\
& + 2(C_{13}C_{23} + C_{12}C_{22})R_x^2\dot{\Phi}\dot{\Theta} - 2(C_{11}C_{22} + C_{12}C_{21})R_xR_y\dot{\Phi}\dot{\Theta}\ldots \\
& - 2(C_{11}C_{23} + C_{13}C_{21})R_xR_z\dot{\Phi}\dot{\Theta} - 2(C_{12}C_{23} + C_{13}C_{22})R_yR_z\dot{\Phi}\dot{\Theta}\ldots \\
& + 2(C_{11}C_{21} + C_{13}C_{23})R_y^2\dot{\Phi}\dot{\Theta} + 2(C_{11}C_{21} + C_{12}C_{22})R_z^2\dot{\Phi}\dot{\Theta} + \left(C_{12}^2 + C_{13}^2\right)R_x^2\dot{\Phi}^2\ldots \\
& - 2C_{11}C_{12}R_xR_y\dot{\Phi}^2 . - 2C_{11}C_{13}R_xR_z\dot{\Phi}^2 - 2C_{12}C_{13}R_yR_z\dot{\Phi}^2 + \left(C_{11}^2 + C_{13}^2\right)R_y^2\dot{\Phi}^2\ldots \\
& + \left(C_{11}^2 + C_{12}^2\right)R_z^2\dot{\Phi}^2
\end{aligned} \tag{64}$$

7.2. Calculation of kinetic energy from a mass point of a pure rotating body (*step 2*)

The energy can also be calculated by the tangential speed vector, preferably within the inertial frame (Eq. (65)):

$$E_{kin} = \frac{1}{2} dm \left[\vec{\omega}_e \times \left(\overline{\mathbf{C}}_b^e \cdot \vec{\mathbf{R}}_m \right) \right]^T \cdot \left[\vec{\omega}_e \times \left(\overline{\mathbf{C}}_b^e \cdot \vec{\mathbf{R}}_m \right) \right] \tag{65}$$

The cross product can be calculated by a so-called skew operator $\tilde{\omega}_e$ (Eq. (32)). So, it is possible to calculate the tangential speed vector of the mass point within the inertial frame:

$$\vec{\mathbf{v}}_{dm} = \tilde{\omega}_e \cdot \overline{\mathbf{C}}_b^e \cdot \vec{\mathbf{R}}_m = \begin{bmatrix} -C_{21}R_x\dot{\Psi} - C_{22}R_y\dot{\Psi} - C_{23}R_z\dot{\Psi} + C_{31}R_x\dot{\Theta} + C_{32}R_y\dot{\Theta} + C_{33}R_z\dot{\Theta} \\ C_{11}R_x\dot{\Psi} + C_{12}R_y\dot{\Psi} + C_{13}R_z\dot{\Psi} - C_{31}R_x\dot{\Phi} - C_{32}R_y\dot{\Phi} - C_{33}R_z\dot{\Phi} \\ -C_{11}R_x\dot{\Theta} - C_{12}R_y\dot{\Theta} - C_{13}R_z\dot{\Theta} + C_{21}R_x\dot{\Phi} + C_{22}R_y\dot{\Phi} + C_{23}R_z\dot{\Phi} \end{bmatrix} \tag{66}$$

From Eq. (66) the square of speed can be calculated (see Eq. (67)):

$$\frac{2E_{kin}}{dm} = v_{dm}^2 = \vec{\mathbf{v}}_{dm}^T \cdot \vec{\mathbf{v}}_{dm} = E_4 + E_5 + E_6 \tag{67}$$

with.

$$\begin{aligned}
E_4 = &\ C_{21}^2 R_x^2 \dot{\Psi}^2 + 2C_{21}C_{22}R_xR_y\dot{\Psi}^2 + 2C_{21}C_{23}R_xR_z\dot{\Psi}^2 - 2C_{21}C_{31}R_x^2\dot{\Theta}\dot{\Psi} \ldots \\
&- 2C_{21}C_{32}R_xR_y\dot{\Theta}\dot{\Psi} - 2C_{21}C_{33}R_xR_z\dot{\Theta}\dot{\Psi} + C_{22}^2 R_y^2\dot{\Psi}^2 + 2C_{22}C_{23}R_yR_z\dot{\Psi}^2 \ldots \\
&- 2C_{22}C_{31}R_xR_y\dot{\Theta}\dot{\Psi} - 2C_{22}C_{32}R_y^2\dot{\Theta}\dot{\Psi} - 2C_{22}C_{33}R_yR_z\dot{\Theta}\dot{\Psi} + C_{23}^2 R_z^2\dot{\Psi}^2 \ldots \\
&- 2C_{23}C_{31}R_xR_z\dot{\Theta}\dot{\Psi} - 2C_{23}C_{32}R_yR_z\dot{\Theta}\dot{\Psi} - 2C_{23}C_{33}R_z^2\dot{\Theta}\dot{\Psi} + C_{31}^2 R_x^2\dot{\Theta}^2 \ldots \\
&+ 2C_{31}C_{32}R_xR_y\dot{\Theta}^2 + 2C_{31}C_{33}R_xR_z\dot{\Theta}^2 + C_{32}^2 R_y^2\dot{\Theta}^2 + 2C_{32}C_{33}R_yR_z\dot{\Theta}^2 + C_{33}^2 R_z^2\dot{\Theta}^2
\end{aligned}$$

$$\begin{aligned}
E_5 = &\ C_{11}^2 R_x^2 \dot{\Psi}^2 + 2C_{11}C_{12}R_xR_y\dot{\Psi}^2 + 2C_{11}C_{13}R_xR_z\dot{\Psi}^2 - 2C_{11}C_{31}R_x^2\dot{\Phi}\dot{\Psi} \ldots \\
&- 2C_{11}C_{32}R_xR_y\dot{\Phi}\dot{\Psi} - 2C_{11}C_{33}R_xR_z\dot{\Phi}\dot{\Psi} + C_{12}^2 R_y^2\dot{\Psi}^2 + 2C_{12}C_{13}R_yR_z\dot{\Psi}^2 \ldots \\
&- 2C_{12}C_{31}R_xR_y\dot{\Phi}\dot{\Psi} - 2C_{12}C_{32}R_y^2\dot{\Phi}\dot{\Psi} - 2C_{12}C_{33}R_yR_z\dot{\Phi}\dot{\Psi} + C_{13}^2 R_z^2\dot{\Psi}^2 \ldots \\
&- 2C_{13}C_{31}R_xR_z\dot{\Phi}\dot{\Psi} - 2C_{13}C_{32}R_yR_z\dot{\Phi}\dot{\Psi} - 2C_{13}C_{33}R_z^2\dot{\Phi}\dot{\Psi} + C_{31}^2 R_x^2\dot{\Phi}^2 \ldots \\
&+ 2C_{31}C_{32}R_xR_y\dot{\Phi}^2 + 2C_{31}C_{33}R_xR_z\dot{\Phi}^2 + C_{32}^2 R_y^2\dot{\Phi}^2 + 2C_{32}C_{33}R_yR_z\dot{\Phi}^2 + C_{33}^2 R_z^2\dot{\Phi}^2
\end{aligned}$$

$$\begin{aligned}
E_6 = &\ C_{11}^2 R_x^2 \dot{\Theta}^2 + 2C_{11}C_{12}R_xR_y\dot{\Theta}^2 + 2C_{11}C_{13}R_xR_z\dot{\Theta}^2 - 2C_{11}C_{21}R_x^2\dot{\Phi}\dot{\Theta} \ldots \\
&- 2C_{11}C_{22}R_xR_y\dot{\Phi}\dot{\Theta} - 2C_{11}C_{23}R_xR_z\dot{\Phi}\dot{\Theta} + C_{12}^2 R_y^2\dot{\Theta}^2 + 2C_{12}C_{13}R_yR_z\dot{\Theta}^2 \ldots \\
&- 2C_{12}C_{21}R_xR_y\dot{\Phi}\dot{\Theta} - 2C_{12}C_{22}R_y^2\dot{\Phi}\dot{\Theta} - 2C_{12}C_{23}R_yR_z\dot{\Phi}\dot{\Theta} + C_{13}^2 R_z^2\dot{\Theta}^2 \ldots \\
&- 2C_{13}C_{21}R_xR_z\dot{\Phi}\dot{\Theta} - 2C_{13}C_{22}R_yR_z\dot{\Phi}\dot{\Theta} - 2C_{13}C_{23}R_z^2\dot{\Phi}\dot{\Theta} + C_{21}^2 R_x^2\dot{\Phi}^2 \ldots \\
&+ 2C_{21}C_{22}R_xR_y\dot{\Phi}^2 + 2C_{21}C_{23}R_xR_z\dot{\Phi}^2 + C_{22}^2 R_y^2\dot{\Phi}^2 + 2C_{22}C_{23}R_yR_z\dot{\Phi}^2 + C_{23}^2 R_z^2\dot{\Phi}^2
\end{aligned}$$

Summarising E_4, E_5 and E_6, follows Eq. (68).

$$\frac{2E_{kin}}{dm} = (C_{11}^2 + C_{21}^2)R_x^2\dot\Psi^2 + 2(C_{11}C_{12} + C_{21}C_{22})R_xR_y\dot\Psi^2 + 2(C_{11}C_{13} + C_{21}C_{23})R_xR_z\dot\Psi^2 \ldots$$
$$+ 2(C_{12}C_{13} + C_{22}C_{23})R_yR_z\dot\Psi^2 + (C_{12}^2 + C_{22}^2)R_y^2\dot\Psi^2 + (C_{13}^2 + C_{23}^2)R_z^2\dot\Psi^2 \ldots$$
$$- 2C_{21}C_{31}R_x^2\dot\Theta\dot\Psi - 2(C_{21}C_{32} + C_{22}C_{31})R_xR_y\dot\Theta\dot\Psi - 2(C_{21}C_{33} + C_{23}C_{31})R_xR_z\dot\Theta\dot\Psi \ldots$$
$$- 2(C_{22}C_{33} + C_{23}C_{32})R_yR_z\dot\Theta\dot\Psi - 2C_{22}C_{32}R_y^2\dot\Theta\dot\Psi - 2C_{23}C_{33}R_z^2\dot\Theta\dot\Psi - 2C_{11}C_{31}R_x^2\dot\Phi\dot\Psi \ldots$$
$$- 2(C_{11}C_{32} + C_{12}C_{31})R_xR_y\dot\Phi\dot\Psi - 2(C_{11}C_{33} + C_{13}C_{31})R_xR_z\dot\Phi\dot\Psi \ldots$$
$$- 2(C_{12}C_{33} + C_{13}C_{32})R_yR_z\dot\Phi\dot\Psi - 2C_{12}C_{32}R_y^2\dot\Phi\dot\Psi - 2C_{13}C_{33}R_z^2\dot\Phi\dot\Psi + (C_{11}^2 + C_{31}^2)R_x^2\dot\Theta^2 \ldots$$
$$+ 2(C_{11}C_{12} + C_{31}C_{32})R_xR_y\dot\Theta^2 + 2(C_{11}C_{13} + C_{31}C_{33})R_xR_z\dot\Theta^2 \ldots$$
$$+ 2(C_{12}C_{13} + C_{32}C_{33})R_yR_z\dot\Theta^2 + (C_{12}^2 + C_{32}^2)R_y^2\dot\Theta^2 + (C_{13}^2 + C_{33}^2)R_z^2\dot\Theta^2 \ldots$$
$$- 2C_{11}C_{21}R_x^2\dot\Phi\dot\Theta - 2(C_{11}C_{22} + C_{12}C_{21})R_xR_y\dot\Phi\dot\Theta - 2(C_{11}C_{23} + C_{13}C_{21})R_xR_z\dot\Phi\dot\Theta \ldots$$
$$- 2(C_{12}C_{23} + C_{13}C_{22})R_yR_z\dot\Phi\dot\Theta - 2C_{12}C_{22}R_y^2\dot\Phi\dot\Theta - 2C_{13}C_{23}R_z^2\dot\Phi\dot\Theta + (C_{21}^2 + C_{31}^2)R_x^2\dot\Phi^2 \ldots$$
$$+ 2(C_{21}C_{22} + C_{31}C_{32})R_xR_y\dot\Phi^2 + 2(C_{21}C_{23} + C_{31}C_{33})R_xR_z\dot\Phi^2 \ldots$$
$$+ 2(C_{22}C_{23} + C_{32}C_{33})R_yR_z\dot\Phi^2 + (C_{22}^2 + C_{32}^2)R_y^2\dot\Phi^2 + (C_{23}^2 + C_{33}^2)R_z^2\dot\Phi^2$$

(68)

7.3. Comparison of the coefficients from both energy calculations for the mass point of pure rotating body (*step 3*)

To show that energy is identical in both approaches (*step 1* and *step 2*), the coefficients of all 36 combinations of lever arms and angular velocities are compared individually with each other in *step 3*. The coefficients of the rotation energy (cf. Eq. (64)) of *step 1* can be found on the left-hand side and the coefficients of kinetic energy (cf. Eq. (68)) of *step2* on the right-hand side. As described previously, the condition of identical energy is only proved, if all coefficients ar equal.

$$C_{32}^2 + C_{33}^2 = C_{11}^2 + C_{21}^2$$
$$R_x^2\dot\Psi^2 : \quad s^2\Phi c^2\Theta + c^2\Phi c^2\Theta = c^2\Theta c^2\Psi + c^2\Theta s^2\Psi$$
$$c^2\Theta = c^2\Theta$$

(69)

$$-2C_{31}C_{32} = 2(C_{11}C_{12} + C_{21}C_{22})$$
$$R_xR_y\dot\Psi^2 : \quad s\Theta c\Theta s\Phi = s\Phi s\Theta c\Theta c^2\Psi - c\Phi c\Theta s\Psi c\Psi + s\Phi s\Theta c\Theta s^2\Psi \ldots$$
$$+ c\Phi c\Theta s\Psi c\Psi$$
$$s\Theta c\Theta s\Phi = s\Phi s\Theta c\Theta$$

(70)

$$-2C_{31}C_{33} = 2(C_{11}C_{13} + C_{21}C_{23})$$
$$R_xR_z\dot\Psi^2 : \quad s\Theta c\Theta c\Phi = c\Psi s\Psi c\Theta s\Phi + c^2\Psi c\Theta s\Theta c\Phi - s\Psi c\Psi c\Theta s\Phi \ldots$$
$$+ s^2\Psi c\Theta s\Theta c\Phi$$
$$s\Theta c\Theta c\Phi = c\Theta s\Theta c\Phi$$

(71)

$$-2C_{32}C_{33} = 2(C_{12}C_{13} + C_{22}C_{23})$$

$$-c^2\Theta s\Phi c\Phi = -s^2\Psi c\Phi s\Phi - s\Psi c\Psi c^2\Phi s\Theta + s\Psi c\Psi s^2\Phi s\Theta\ldots$$

$$+ c^2\Psi s^2\Theta s\Phi c\Phi - c^2\Psi c\Phi s\Phi + s\Psi c\Psi c^2\Phi s\Theta\ldots$$

$$R_y R_z \dot{\Psi}^2: \qquad - s\Psi c\Psi s^2\Phi s\Theta + s^2\Psi s^2\Theta s\Phi c\Phi \tag{72}$$

$$= -1 \cdot c\Phi s\Phi + s^2\Theta s\Phi c\Phi$$

$$-c^2\Theta s\Phi c\Phi = -c^2\Theta s\Phi c\Phi$$

$$C_{31}^2 + C_{33}^2 = C_{12}^2 + C_{22}^2$$

$$s^2\Theta + c^2\Theta c^2\Phi = s^2\Psi c^2\Phi - 2s\Psi c\Psi s\Theta c\Phi s\Phi + c^2\Psi s^2\Theta s^2\Phi\ldots$$

$$+ c^2\Psi c^2\Phi + 2s\Psi c\Psi s\Theta s\Phi c\Phi + s^2\Phi s^2\Theta s^2\Psi$$

$$R_y^2 \dot{\Psi}^2: \qquad = c^2\Phi + s^2\Theta s^2\Phi = c^2\Phi \cdot 1 + s^2\Theta s^2\Phi \tag{73}$$

$$= c^2\Phi c^2\Theta + c^2\Phi s^2\Theta + s^2\Theta \cdot 1 - s^2\Theta c^2\Phi$$

$$s^2\Theta + c^2\Theta c^2\Phi = c^2\Phi c^2\Theta + s^2\Theta$$

$$C_{31}^2 + C_{32}^2 = C_{13}^2 + C_{23}^2$$

$$s^2\Theta + c^2\Theta s^2\Phi = s^2\Psi s^2\Phi + 2s\Psi c\Psi s\Theta s\Phi c\Phi + c^2\Psi s^2\Theta c^2\Phi\ldots$$

$$+ c^2\Psi s^2\Phi - 2s\Psi c\Psi s\Theta s\Phi c\Phi + s^2\Theta s^2\Psi c^2\Phi$$

$$R_z^2 \dot{\Psi}^2: \qquad = s^2\Phi + s^2\Theta c^2\Phi = s^2\Phi \cdot 1 + s^2\Theta c^2\Phi \tag{74}$$

$$= s^2\Phi c^2\Theta + s^2\Phi s^2\Theta + s^2\Theta \cdot 1 - s^2\Theta s^2\Phi$$

$$s^2\Theta + c^2\Theta s^2\Phi = s^2\Phi c^2\Theta + s^2\Theta$$

$$2(C_{22}C_{32} + C_{23}C_{33}) = -2C_{21}C_{31}$$

$$R_x^2 \dot{\Theta}\dot{\Psi}: c\Psi c\Theta s\Phi c\Phi + s\Psi s\Theta c\Theta s^2\Phi - c\Psi c\Theta s\Phi c\Phi. + s\Psi s\Theta c\Theta c^2\Phi = s\Psi c\Theta s\Theta \tag{75}$$

$$s\Psi s\Theta c\Theta = s\Psi c\Theta s\Theta$$

$$R_x R_y \dot{\Theta}\dot{\Psi}: - 2(C_{22}C_{31} + C_{21}C_{32}) = -2(C_{21}C_{32} + C_{22}C_{31}) \tag{76}$$

$$R_x R_z \dot{\Theta}\dot{\Psi}: - 2(C_{21}C_{33} + C_{23}C_{31}) = -2(C_{21}C_{33} + C_{23}C_{31}) \tag{77}$$

$$R_y R_z \dot{\Theta}\dot{\Psi}: - 2(C_{22}C_{33} + C_{23}C_{32}) = -2(C_{22}C_{33} + C_{23}C_{32}) \tag{78}$$

$$2(C_{23}C_{33} + C_{21}C_{31}) = -2C_{22}C_{32}$$

$$-c\Psi c\Theta s\Phi c\Phi + s\Psi s\Theta c\Theta c^2\Phi - s\Psi s\Theta c\Theta = -c\Psi c\Theta c\Phi s\Phi - s\Psi c\Theta s\Theta s^2\Phi$$

$$R_y^2 \dot{\Theta}\dot{\Psi}: \qquad \qquad \qquad \qquad \tag{79}$$

$$s\Psi s\Theta c\Theta (1 - s^2\Phi - 1) = -s\Psi c\Theta s\Theta s^2\Phi$$

$$-s\Psi c\Theta s\Theta s^2\Phi = -s\Psi c\Theta s\Theta s^2\Phi$$

$$2(C_{22}C_{32} + C_{21}C_{31}) = -2C_{23}C_{33}$$

$$R_z^2\dot{\Theta}\dot{\Psi}: \quad c\Psi c\Theta s\Phi c\Phi + s\Psi s\Theta c\Theta s^2\Phi - s\Psi s\Theta c\Theta = c\Psi c\Theta s\Phi c\Phi - s\Psi s\Theta c\Theta c^2\Phi$$

$$s\Psi s\Theta c\Theta(1 - c^2\Phi - 1) = -s\Psi c\Theta s\Theta c^2\Phi \tag{80}$$

$$-s\Psi c\Theta s\Theta c^2\Phi = -s\Psi c\Theta s\Theta c^2\Phi$$

$$2(C_{13}C_{33} + C_{12}C_{32}) = -2C_{11}C_{31}$$

$$R_x^2\dot{\Phi}\dot{\Psi}: \quad \begin{pmatrix} s\Psi c\Theta s\Phi c\Phi + c\Psi s\Theta c\Theta c^2\Phi - s\Psi c\Theta s\Phi c\Phi \ldots \\ +c\Psi s\Theta c\Theta s^2\Phi \end{pmatrix} = c\Psi c\Theta s\Theta \tag{81}$$

$$c\Psi s\Theta c\Theta = c\Psi c\Theta s\Theta$$

$$R_x R_y \dot{\Phi}\dot{\Psi}: \quad -2(C_{12}C_{31} + C_{11}C_{32}) = -2(C_{11}C_{32} + C_{12}C_{31}) \tag{82}$$

$$R_x R_z \dot{\Phi}\dot{\Psi}: \quad -2(C_{11}C_{33} + C_{13}C_{31}) = -2(C_{11}C_{33} + C_{13}C_{31}) \tag{83}$$

$$R_y R_z \dot{\Phi}\dot{\Psi}: \quad -2(C_{12}C_{33} + C_{13}C_{32}) = -2(C_{12}C_{33} + C_{13}C_{32}) \tag{84}$$

$$2(C_{13}C_{33} + C_{11}C_{31}) = -2C_{12}C_{32}$$

$$R_y^2\dot{\Phi}\dot{\Psi}: \quad s\Psi c\Theta s\Phi c\Phi + c\Psi s\Theta c\Theta c^2\Phi - c\Psi c\Theta s\Theta = s\Psi c\Theta s\Phi c\Phi - c\Psi s\Theta c\Theta s^2\Phi$$

$$c\Psi s\Theta c\Theta(1 - s^2\Phi - 1) = -c\Psi s\Theta c\Theta s^2\Phi \tag{85}$$

$$-c\Psi s\Theta c\Theta s^2\Phi = -c\Psi s\Theta c\Theta s^2\Phi$$

$$2(C_{12}C_{32} + C_{11}C_{31}) = -2C_{13}C_{33}$$

$$R_z^2\dot{\Phi}\dot{\Psi}: \quad -s\Psi c\Theta s\Phi c\Phi + c\Psi s\Theta c\Theta s^2\Phi - c\Psi c\Theta s\Theta = -s\Psi c\Theta s\Phi c\Phi - c\Psi s\Theta c\Theta c^2\Phi$$

$$c\Psi s\Theta c\Theta(1 - c^2\Phi - 1) = -c\Psi s\Theta c\Theta c^2\Phi \tag{86}$$

$$-c\Psi s\Theta c\Theta c^2\Phi = -c\Psi s\Theta c\Theta c^2\Phi$$

$$C_{22}^2 + C_{23}^2 = C_{11}^2 + C_{31}^2$$

$$R_x^2\dot{\Theta}^2: \quad \begin{pmatrix} c^2\Psi c^2\Phi + 2s\Psi c\Psi s\Theta s\Phi c\Phi + s^2\Phi s^2\Theta s^2\Psi \ldots \\ +c^2\Psi s^2\Phi - 2s\Psi c\Psi s\Theta s\Phi c\Phi + s^2\Theta s^2\Psi c^2\Phi \end{pmatrix} = c^2\Psi c^2\Theta + s^2\Theta$$

$$c^2\Psi + s^2\Theta s^2\Psi = \tag{87}$$

$$c^2\Psi \cdot 1 + s^2\Theta s^2\Psi =$$

$$c^2\Psi s^2\Theta + c^2\Psi c^2\Theta + s^2\Theta \cdot 1 - s^2\Theta c^2\Psi =$$

$$c^2\Psi c^2\Theta + s^2\Theta = c^2\Psi c^2\Theta + s^2\Theta$$

$$-2C_{21}C_{22} = 2(C_{11}C_{12} + C_{31}C_{32})$$

$$R_x R_y \dot{\Theta}^2: \quad -s\Psi c\Psi c\Theta c\Phi - s^2\Psi c\Theta s\Theta s\Phi = -c\Psi s\Psi c\Theta c\Phi + c^2\Psi s\Theta c\Theta s\Phi - s\Theta c\Theta s\Phi$$

$$-s^2\Psi c\Theta s\Theta s\Phi = (1 - s^2\Psi - 1)s\Theta c\Theta s\Phi \tag{88}$$

$$-s^2\Psi c\Theta s\Theta s\Phi = -s^2\Psi s\Theta c\Theta s\Phi$$

$$-2C_{21}C_{23} = 2(C_{11}C_{13} + C_{31}C_{33})$$

$$R_x R_z \dot{\Theta}^2: \quad s\Psi c\Psi c\Theta s\Phi - s^2\Psi s\Theta c\Theta c\Phi = s\Psi c\Psi c\Theta s\Phi + c^2\Psi c\Theta s\Theta c\Phi - s\Theta c\Theta c\Phi$$

$$-s^2\Psi s\Theta c\Theta c\Phi = (1 - s^2\Psi - 1)s\Theta c\Theta c\Phi$$

$$-s^2\Psi s\Theta c\Theta c\Phi = -s^2\Psi s\Theta c\Theta c\Phi$$

(89)

$$-2C_{22}C_{23} = 2(C_{12}C_{13} + C_{32}C_{33})$$

$$\begin{pmatrix} c^2\Psi s\Theta c\Phi - s\Psi c\Psi s\Theta c^2\Phi \ldots \\ + s\Psi c\Psi s\Theta s^2\Phi - s^2\Psi s^2\Theta s\Phi c\Phi \end{pmatrix} = \begin{pmatrix} -s^2\Psi s\Phi c\Phi - s\Psi c\Psi s\Theta c^2\Phi \ldots \\ + s\Psi c\Psi s\Theta s^2\Phi + c^2\Psi s^2\Theta s\Phi c\Phi \ldots \\ + c^2\Theta s\Phi c\Phi \end{pmatrix}$$

$$R_y R_z \dot{\Theta}^2: \quad c^2\Psi s\Theta c\Phi - s^2\Psi s^2\Theta s\Phi c\Phi = \begin{pmatrix} -s^2\Psi s\Phi c\Phi + c^2\Psi s^2\Theta s\Phi c\Phi \ldots \\ + c^2\Theta s\Phi c\Phi \end{pmatrix}$$

(90)

$$s\Phi c\Phi(c^2\Psi - s^2\Psi s^2\Theta) = s\Phi c\Phi(-s^2\Psi + c^2\Psi s^2\Theta + c^2\Theta)$$

$$c^2\Psi - s^2\Psi s^2\Theta = -s^2\Psi + c^2\Psi s^2\Theta + c^2\Theta$$

$$1 - s^2\Psi - s^2\Theta + c^2\Psi s^2\Theta =$$

$$-s^2\Psi + c^2\Theta + c^2\Psi s^2\Theta = -s^2\Psi + c^2\Psi s^2\Theta + c^2\Theta$$

$$C_{21}^2 + C_{23}^2 = C_{12}^2 + C_{32}^2$$

$$\begin{pmatrix} s^2\Psi c^2\Theta + c^2\Psi s^2\Phi \ldots \\ -2s\Psi c\Psi s\Theta s\Phi c\Phi \ldots \\ + s^2\Psi s^2\Theta c^2\Phi \end{pmatrix} = \begin{pmatrix} s^2\Psi c^2\Phi - 2s\Psi c\Psi s\Theta s\Phi c\Phi \ldots \\ + c^2\Psi s^2\Theta s^2\Phi + c^2\Theta s^2\Phi \end{pmatrix}$$

$$R_y^2 \dot{\Theta}^2: \quad \begin{pmatrix} s^2\Psi c^2\Theta + c^2\Psi s^2\Phi \ldots \\ + s^2\Psi s^2\Theta c^2\Phi \end{pmatrix} = \begin{pmatrix} s^2\Psi c^2\Phi + c^2\Psi s^2\Theta s^2\Phi \ldots \\ + c^2\Theta s^2\Phi \end{pmatrix}$$

(91)

$$\begin{pmatrix} s^2\Psi c^2\Theta \cdot 1 + c^2\Psi \cdot 1 \cdot s^2\Phi \ldots \\ + s^2\Psi s^2\Theta c^2\Phi \end{pmatrix} = \begin{pmatrix} s^2\Psi \cdot 1 \cdot c^2\Phi + c^2\Psi s^2\Theta s^2\Phi \ldots \\ + 1 \cdot c^2\Theta s^2\Phi \end{pmatrix}$$

$$\begin{pmatrix} s^2\Psi c^2\Theta s^2\Phi_1 + s^2\Psi c^2\Theta c^2\Phi_2 \ldots \\ + c^2\Psi s^2\Theta s^2\Phi_3 + c^2\Psi c^2\Theta s^2\Phi_4 \ldots \\ + s^2\Psi s^2\Theta c^2\Phi_5 \end{pmatrix} = \begin{pmatrix} s^2\Psi s^2\Theta c^2\Phi_5 + s^2\Psi c^2\Theta c^2\Phi_2 \ldots \\ + c^2\Psi s^2\Theta s^2\Phi_3 + s^2\Psi c^2\Theta s^2\Phi_1 \ldots \\ + c^2\Psi c^2\Theta s^2\Phi_4 \end{pmatrix}$$

$$C_{21}^2 + C_{22}^2 = C_{13}^2 + C_{33}^2$$

$$\begin{pmatrix} s^2\Psi c^2\Theta + c^2\Psi c^2\Phi \ldots \\ + 2s\Psi c\Psi s\Theta s\Phi c\Phi + s^2\Psi s^2\Theta s^2\Phi \end{pmatrix} = \begin{pmatrix} s^2\Psi s^2\Phi + 2s\Psi c\Psi s\Theta s\Phi c\Phi \ldots \\ + c^2\Psi s^2\Theta c^2\Phi + c^2\Theta c^2\Phi \end{pmatrix}$$

$$s^2\Psi c^2\Theta + c^2\Psi c^2\Phi + s^2\Psi s^2\Theta s^2\Phi = s^2\Psi s^2\Phi + c^2\Psi s^2\Theta c^2\Phi + c^2\Theta c^2\Phi$$

$$R_z^2 \dot{\Theta}^2: \quad \begin{pmatrix} s^2\Psi c^2\Theta \cdot 1 + c^2\Psi \cdot 1 \cdot c^2\Phi \ldots \\ + s^2\Psi s^2\Theta s^2\Phi \end{pmatrix} = \begin{pmatrix} s^2\Psi \cdot 1 \cdot s^2\Phi + c^2\Psi s^2\Theta c^2\Phi \ldots \\ + 1 \cdot c^2\Theta c^2\Phi \end{pmatrix}$$

(92)

$$\begin{pmatrix} s^2\Psi c^2\Theta s^2\Phi_1 + s^2\Psi c^2\Theta c^2\Phi_2 \ldots \\ + c^2\Psi s^2\Theta c^2\Phi_3 + c^2\Psi c^2\Theta c^2\Phi_4 \ldots \\ + s^2\Psi s^2\Theta s^2\Phi_5 \end{pmatrix} = \begin{pmatrix} s^2\Psi s^2\Theta s^2\Phi_5 + s^2\Psi c^2\Theta s^2\Phi_1 \ldots \\ + c^2\Psi s^2\Theta c^2\Phi_3 + s^2\Psi c^2\Theta c^2\Phi_2 \ldots \\ + c^2\Psi c^2\Theta c^2\Phi_4 \end{pmatrix}$$

$$2(C_{13}C_{23} + C_{12}C_{22}) = -2C_{11}C_{21}$$

$$R_x^2 \dot{\Phi}\dot{\Theta}: \begin{pmatrix} -s\Psi c\Psi s^2\Phi + s^2\Psi s\Theta s\Phi c\Phi - c^2\Psi s\Theta s\Phi c\Phi + s\Psi c\Psi s^2\Theta c^2\Phi \ldots \\ -s\Psi c\Psi c^2\Phi - s^2\Psi s\Theta s\Phi c\Phi + c^2\Psi s\Theta s\Phi c\Phi + s\Psi c\Psi s^2\Theta s^2\Phi \end{pmatrix} = -c\Psi s\Psi c^2\Theta$$

$$-s\Psi c\Psi s^2\Phi + s\Psi c\Psi s^2\Theta c^2\Phi - s\Psi c\Psi c^2\Phi + s\Psi c\Psi s^2\Theta s^2\Phi =$$
$$-s\Psi c\Psi + s\Psi c\Psi s^2\Theta =$$
$$s\Psi c\Psi\left(-1 + 1 - c^2\Theta\right) =$$
$$-s\Psi c\Psi c^2\Theta = -c\Psi s\Psi c^2\Theta$$

(93)

$$R_x R_y \dot{\Phi}\dot{\Theta}: -2(C_{11}C_{22} + C_{12}C_{21}) = -2(C_{11}C_{22} + C_{12}C_{21})$$

(94)

$$R_x R_z \dot{\Phi}\dot{\Theta}: -2(C_{11}C_{23} + C_{13}C_{21}) = -2(C_{11}C_{23} + C_{13}C_{21})$$

(95)

$$R_y R_z \dot{\Phi}\dot{\Theta}: -2(C_{12}C_{23} + C_{13}C_{22}) = -2(C_{12}C_{23} + C_{13}C_{22})$$

(96)

$$2(C_{11}C_{21} + C_{13}C_{23}) = -2C_{12}C_{22}$$

$$R_y^2 \dot{\Phi}\dot{\Theta}: \begin{pmatrix} c\Psi s\Psi c^2\Theta - s\Psi c\Psi s^2\Phi + s^2\Psi s\Theta s\Phi c\Phi \ldots \\ -c^2\Psi s\Theta s\Phi c\Phi + s\Psi c\Psi s^2\Theta c^2\Phi \end{pmatrix} = \begin{pmatrix} s\Psi c\Psi c^2\Phi + s^2\Psi s\Theta s\Phi c\Phi \ldots \\ -c^2\Psi s\Theta s\Phi c\Phi - s\Psi c\Psi s^2\Theta s^2\Phi \end{pmatrix}$$

$$c\Psi s\Psi c^2\Theta - s\Psi c\Psi s^2\Phi + s\Psi c\Psi s^2\Theta c^2\Phi = s\Psi c\Psi c^2\Phi - s\Psi c\Psi s^2\Theta s^2\Phi$$
$$s\Psi c\Psi\left(c^2\Theta - s^2\Phi + s^2\Theta c^2\Phi\right) = s\Psi c\Psi\left(c^2\Phi - s^2\Theta s^2\Phi\right)$$
$$c^2\Theta - s^2\Phi + s^2\Theta c^2\Phi = c^2\Phi - s^2\Theta s^2\Phi$$
$$1 - s^2\Theta - 1 + c^2\Phi + s^2\Theta c^2\Phi =$$
$$c^2\Phi + s^2\Theta\left(-1 + c^2\Phi\right) =$$
$$c^2\Phi + s^2\Theta\left(-1 + 1 - s^2\Phi\right) =$$
$$c^2\Phi - s^2\Theta s^2\Phi = c^2\Phi - s^2\Theta s^2\Phi$$

(97)

$$2(C_{11}C_{21} + C_{12}C_{22}) = -2C_{13}C_{23}$$

$$R_z^2 \dot{\Phi}\dot{\Theta}: \begin{pmatrix} s\Psi c\Psi c^2\Theta - s\Psi c\Psi c^2\Phi \ldots \\ -s^2\Psi s\Theta s\Phi c\Phi + c^2\Psi s\Theta s\Phi c\Phi \ldots \\ +s\Psi c\Psi s^2\Theta s^2\Phi \end{pmatrix} = \begin{pmatrix} s\Psi c\Psi s^2\Phi - s^2\Psi s\Theta s\Phi c\Phi \ldots \\ +c^2\Psi s\Theta s\Phi c\Phi - s\Psi c\Psi s^2\Theta c^2\Phi \end{pmatrix}$$

$$c\Psi s\Psi c^2\Theta - s\Psi c\Psi c^2\Phi + s\Psi c\Psi s^2\Theta s^2\Phi = s\Psi c\Psi s^2\Phi - s\Psi c\Psi s^2\Theta c^2\Phi$$

$$s\Psi c\Psi\left(c^2\Theta - c^2\Phi + s^2\Theta s^2\Phi\right) = s\Psi c\Psi\left(s^2\Phi - s^2\Theta c^2\Phi\right)$$
$$c^2\Theta - c^2\Phi + s^2\Theta s^2\Phi = s^2\Phi - s^2\Theta c^2\Phi$$
$$1 - s^2\Theta - 1 + s^2\Phi + s^2\Theta s^2\Phi =$$
$$s^2\Phi + s^2\Theta\left(-1 + s^2\Phi\right) =$$
$$s^2\Phi + s^2\Theta\left(-1 + 1 - c^2\Phi\right) =$$
$$s^2\Phi - s^2\Theta c^2\Phi = s^2\Phi - s^2\Theta c^2\Phi$$

(98)

$$C_{12}^2 + C_{13}^2 = C_{21}^2 + C_{31}^2$$

$$R_x^2\dot{\Phi}^2: \quad \begin{pmatrix} s^2\Psi c^2\Phi - 2s\Psi c\Psi s\Theta s\Phi c\Phi \\ + c^2\Psi s^2\Theta s^2\Phi + s^2\Psi s^2\Phi \ldots \\ + 2s\Psi c\Psi s\Theta s\Phi c\Phi + c^2\Psi s^2\Theta c^2\Phi \end{pmatrix} = s^2\Psi c^2\Theta + s^2\Theta$$

$$\begin{pmatrix} s^2\Psi c^2\Phi + c^2\Psi s^2\Theta s^2\Phi + s^2\Psi s^2\Phi \ldots \\ + c^2\Psi s^2\Theta c^2\Phi \end{pmatrix} = \tag{99}$$

$$s^2\Psi + c^2\Psi s^2\Theta =$$

$$s^2\Psi \cdot 1 + \left(1 - s^2\Psi\right)s^2\Theta =$$

$$s^2\Psi s^2\Theta + s^2\Psi c^2\Theta + s^2\Theta - s^2\Psi s^2\Theta =$$

$$s^2\Psi c^2\Theta + s^2\Theta = s^2\Psi c^2\Theta + s^2\Theta$$

$$-2C_{11}C_{12} = 2(C_{21}C_{22} + C_{31}C_{32})$$

$$R_xR_y\dot{\Phi}^2: \quad s\Psi c\Psi c\Theta c\Phi - c^2\Psi c\Theta s\Theta s\Phi = c\Psi s\Psi c\Theta c\Phi + s^2\Psi s\Theta c\Theta s\Phi - s\Theta c\Theta s\Phi$$

$$-c^2\Psi c\Theta s\Theta s\Phi = \left(1 - c^2\Psi - 1\right)s\Theta c\Theta s\Phi \tag{100}$$

$$-c^2\Psi c\Theta s\Theta s\Phi = -c^2\Psi s\Theta c\Theta s\Phi$$

$$-2C_{11}C_{13} = 2(C_{21}C_{23} + C_{31}C_{33})$$

$$R_xR_z\dot{\Phi}^2: \quad -s\Psi c\Psi c\Theta s\Phi - c^2\Psi s\Theta c\Theta c\Phi = -s\Psi c\Psi c\Theta s\Phi + s^2\Psi s\Theta c\Theta c\Phi - s\Theta c\Theta c\Phi$$

$$-c^2\Psi c\Theta s\Theta c\Phi = \left(1 - c^2\Psi - 1\right)s\Theta c\Theta c\Phi \tag{101}$$

$$-c^2\Psi c\Theta s\Theta c\Phi = -c^2\Psi s\Theta c\Theta c\Phi$$

$$-2C_{12}C_{13} = 2(C_{22}C_{23} + C_{32}C_{33})$$

$$R_yR_z\dot{\Phi}^2: \quad \begin{pmatrix} s^2\Psi s\Phi c\Phi + s\Psi c\Psi s\Theta c^2\Phi \ldots \\ -s\Psi c\Psi s\Theta s^2\Phi - c^2\Psi s^2\Theta s\Phi c\Phi \end{pmatrix} = \begin{pmatrix} -c^2\Psi s\Phi c\Phi + s\Psi c\Psi s\Theta c^2\Phi \ldots \\ -s\Psi c\Psi s\Theta s^2\Phi + s^2\Psi s^2\Theta s\Phi c\Phi \ldots \\ + c^2\Theta s\Phi c\Phi \end{pmatrix}$$

$$s\Phi c\Phi\left(s^2\Psi - c^2\Psi s^2\Theta\right) = s\Phi c\Phi\left(-c^2\Psi + s^2\Psi s^2\Theta + c^2\Theta\right) \tag{102}$$

$$s^2\Psi - c^2\Psi s^2\Theta = -c^2\Psi + s^2\Psi s^2\Theta + c^2\Theta$$

$$= -1 + s^2\Psi + s^2\Psi s^2\Theta + 1 - s^2\Theta$$

$$= s^2\Psi + s^2\Theta\left(1 - c^2\Psi - 1\right)$$

$$s^2\Psi - c^2\Psi s^2\Theta = s^2\Psi - s^2\Theta c^2\Psi$$

$$C_{11}^2 + C_{13}^2 = C_{22}^2 + C_{32}^2$$

$$\begin{pmatrix} c^2\Psi c^2\Theta + s^2\Psi s^2\Phi \dots \\ + 2s\Psi c\Psi s\Theta s\Phi c\Phi + c^2\Psi s^2\Theta c^2\Phi \end{pmatrix} = \begin{pmatrix} c^2\Psi c^2\Phi + 2s\Psi c\Psi s\Theta s\Phi c\Phi \dots \\ + s^2\Psi s^2\Theta s^2\Phi + c^2\Theta s^2\Phi \end{pmatrix}$$

$$c^2\Psi c^2\Theta + s^2\Psi s^2\Phi + c^2\Psi s^2\Theta c^2\Phi = c^2\Psi c^2\Phi + s^2\Psi s^2\Theta s^2\Phi + c^2\Theta s^2\Phi$$

$$R_y^2\dot{\Phi}^2 : \quad \begin{pmatrix} c^2\Psi c^2\Theta \cdot 1 + s^2\Psi \cdot 1 \cdot s^2\Phi \dots \\ + c^2\Psi s^2\Theta c^2\Phi \end{pmatrix} = \begin{pmatrix} c^2\Psi \cdot 1 \cdot c^2\Phi + s^2\Psi s^2\Theta s^2\Phi \dots \\ + 1 \cdot c^2\Theta s^2\Phi \end{pmatrix} \quad (103)$$

$$\begin{pmatrix} c^2\Psi c^2\Theta s^2\Phi_1 + c^2\Psi c^2\Theta c^2\Phi_2 \dots \\ + s^2\Psi s^2\Theta s^2\Phi_3 + s^2\Psi c^2\Theta s^2\Phi_4 \\ + c^2\Psi s^2\Theta c^2\Phi_5 \end{pmatrix} = \begin{pmatrix} c^2\Psi s^2\Theta c^2\Phi_5 + c^2\Psi c^2\Theta c^2\Phi_2 \dots \\ + s^2\Psi s^2\Theta s^2\Phi_3 + s^2\Psi c^2\Theta s^2\Phi_4 \dots \\ + c^2\Psi c^2\Theta s^2\Phi_1 \end{pmatrix}$$

$$C_{11}^2 + C_{12}^2 = C_{23}^2 + C_{33}^2$$

$$\begin{pmatrix} c^2\Psi c^2\Theta + s^2\Psi c^2\Phi \dots \\ - 2s\Psi c\Psi s\Theta s\Phi c\Phi + c^2\Psi s^2\Theta s^2\Phi \end{pmatrix} = \begin{pmatrix} c^2\Psi s^2\Phi - 2s\Psi c\Psi s\Theta s\Phi c\Phi \dots \\ + s^2\Psi s^2\Theta c^2\Phi + c^2\Theta c^2\Phi \end{pmatrix}$$

$$R_z^2\dot{\Phi}^2 : \quad c^2\Psi c^2\Theta + s^2\Psi c^2\Phi + c^2\Psi s^2\Theta s^2\Phi = c^2\Psi s^2\Phi + s^2\Psi s^2\Theta c^2\Phi + c^2\Theta c^2\Phi$$

$$\begin{pmatrix} c^2\Psi c^2\Theta \cdot 1 + s^2\Psi \cdot 1 \cdot c^2\Phi \dots \\ + c^2\Psi s^2\Theta s^2\Phi \end{pmatrix} = \begin{pmatrix} c^2\Psi \cdot 1 \cdot s^2\Phi + s^2\Psi s^2\Theta c^2\Phi \dots \\ + 1 \cdot c^2\Theta c^2\Phi \end{pmatrix}$$

$$\begin{pmatrix} c^2\Psi c^2\Theta s^2\Phi_1 + c^2\Psi c^2\Theta c^2\Phi_2 \dots \\ + s^2\Psi s^2\Theta c^2\Phi_3 + s^2\Psi c^2\Theta c^2\Phi_4 \dots \\ + c^2\Psi s^2\Theta s^2\Phi_5 \end{pmatrix} = \begin{pmatrix} c^2\Psi s^2\Theta s^2\Phi_5 + c^2\Psi c^2\Theta s^2\Phi_1 \dots \\ + s^2\Psi s^2\Theta c^2\Phi_3 + s^2\Psi c^2\Theta c^2\Phi_4 \dots \\ + c^2\Psi c^2\Theta c^2\Phi_2 \end{pmatrix} \quad (104)$$

The previous calculation demonstrated the validity of Eq. (35).

8. Conclusion

This work presents the method of inertial value transformation for maritime applications. Firstly, an introduction in irregular seas and an overview of ships degrees of freedom are given. In the following section, the traditional Kirchhoff motion equations in the body-fixed reference frame are introduced, which represent a hydrodynamic affected Eulerian gyro tied up a Newtonian body within the body-fixed view. The formal derivation of motion equations of a free-floating body in inertial coordinate system is presented in the main part. It is shown that the transformation of the equations into the body-fixed system leads to the well-known Kirchhoff motion equations. 6DOF simulations for a crew transfer vessel in head seas and

beam seas illustrate the comparison of motions in both reference systems. It is mentioned that temporal integration of the motion equations in inertial system leads to unstable and chaotic motions of the ship. Rebuilding the Eulerian gyro at first within the project SOOP [6], Korte et al. [24] by introducing an additional and opposite directed transformation of the rotational accelerations, the present work shows their general applicability and necessity for free-moving bodies (6DOF) within inertial frame. By its consequent use, the motion behaviour of the ship can be stabilised over longer periods. A proof presents the energy conservation of inertia value transformation for a rotating body. Finally, the contribution has shown a failure in common motion calculation practice for vehicles.

The intention of motion equations in inertial reference system is the simulation of mechanically coupled multibody systems in seas. To analyse the interaction effects, the forces and moments of all included bodies have to be defined in the same reference system. This requires a transformation of the motion equations that can be realised with the presented method of inertia value transformation. For a multibody system, a CTV is fixed at the bow to an offshore wind turbine tower and can make ideal rotations; the method including the additional transformation leads to a stable system. The scenario describes the interaction of a fixed and a floating body. Further investigations in the field of multibody dynamics are planned for the future. A scenario of two ships, which are mechanically coupled in tandem and rotate ideally, is developed currently. The challenge in comparison to the first multibody system is the interaction of two floating bodies. Other applications of the method, which are planned in further work of the authors, are simulations of offshore crane processes or 3D simulations of a ROV, which is coupled to a mother ship via umbilical. For the parameterisation of controllers, the question of the real-time application is still in focus of research.

Acknowledgements

Author details

Holger Korte[1]*, Sven Stuppe[1], Jan-Hendrik Wesuls[1] and Tsutomu Takagi[2]

*Address all correspondence to: holger.korte@jade-hs.de

1 Department of Maritime and Logistics Studies Elsfleth, Jade University of Applied Sciences Wilhelmshaven/Oldenburg/Elsfleth, Elsfleth, Germany

2 Graduate School of Fisheries Sciences, Hokkaido University, Hakodate, Japan

References

[1] Fossen TI. Handbook of Marine Craft Hydrodynamics and Motion Control. 1st ed. Chichester UK: J. Wiley & Sons; 1994. DOI: ISBN 0 471 94113 1

[2] Korte H, Takagi T. Dynamic motion calculation of a flexible structure using inertia transformation algorithm. In: Workshop on Fishing and Marine Production Technology; 9-10. August; Trondheim. NTNU. 2004. pp. 1-11. DOI: 10.13140/RG.2.1.4006.4724

[3] Kirchhoff G. Über die Bewegung eines Rotationskörpers in einer Flüssigkeit. Crelles Journal. 1869;**71**:237-273

[4] Wendel K. Hydrodynamische Massen und hydrodynamische Massenträgheitsmomente. Jahrbuch der Schiffbautechnischen Gesellschaft. 1950;207-255

[5] Korte H, Takagi T. Transformation von Trägheitsgrößen zur Lösung der Mehrkörperdynamik in der Meerestechnik. In: 101. Jahrbuch der Schiffbautechnischen Gesellschaft. Hamburg: Schiffahrts-Verlag "Hansa"; 2007. pp. 313-325

[6] Korte H. Track control of a towed underwater sensor carrier. In: IFAC Control in Transportation Systems. Braunschweig: IFAC; 2000. pp. 89-94

[7] Paschen M. Contribution to Predict Trajectories of Pelagic Fishing Gears Affected by Ship Manoeuvres (in German) [Dissertation]. Rostock: University of Rostock; 1982

[8] Suzuki K, Takagi T, Shimizu T, Hiraishi T, Yamamoto K, Nashimoto K. Validity and visualization of a numerical model used to determine dynamic configuration of fishing net. Fisheries Science. 2003;**69**(4):1-18. DOI: 10.1046/j.1444-2906.2003.00676.x · Source: OAI

[9] Aamo O, Fossen TI. Finite element modelling of moored vessels. Mathematical and Computer Modelling of Dynamical Systems. 2001;**7**(1):47-75

[10] Abreu P, Morishita H, Pascoal A, Ribero J, Silva H. Marine vehicles with streamers for geotechnical surveys: Modeling, positioning and control. In: 10th IFAC CAMS; September; Trondheim. IFAC-PapersOnLine 49-23; 2016. p. 458-464

[11] Berntsen P, Aamo O, Leira B, Sørensen A. Structural reliability - based control of moored interconnected structures. Control Engineering Practice. 2008;**16**(4):495-504

[12] Korte H. Motion modelling of a manoeuvring ship at anchor in flowing waters. In: Yamane T, editor. Contributions on the Theory of Fishing Gears and Related Marine Systems; 5.-7. November; University of Kinki, Nara (Jp). Nara:2009. pp. 207-216. DOI: ISBN 4-946-421-13-6

[13] Yang K, Wang X, Wu C. Simulation platform for the underwater snakelike robot swimming based on Kane's dynamic model and central pattern generator. Journal Shanghai Jiaotong University. 2014;**19**(3):294-301

[14] Kane TR, Levison DA. Dynamics: Theory and Applications. 1st ed. New York: McGraw-Hill; 1985

[15] Takagi T, Miyata S, Fusejima I, Oshima T, Uehara T, Suzuki K, Nomura Y, Kanechiku M, Torisawa S. Potential of computer simulation for buoy-line type of purse seine fishing. In: Paschen M, editors. Contributions on the Theory of Fishing Gears and Related Marine Systems; 9-12. Ocktober; Rostock. Aachen: Shaker Verlag; 2013. p. 55-62. DOI: ISBN 978-3-8440-2251-3

[16] Korte H, Stuppe S, Wesuls J-H, Takagi T. Application of the inertia value transformation to simulate the transfer scenario of service staff from a crew transfer vessel to offshore wind turbines. In: Paschen M, O'Neil FG, Ivanovic A, editors. Contributions on the theory of fishing gears and related marine systems; 27-29. October; Aberdeen. Aachen: Shaker Verlag; 2015. p. 227-237. DOI: ISBN 978-3-8440-3955-9

[17] Korte H, Wesuls J-H, Stuppe S, Takagi T. Towards an approach to 6 DOF inertial kinematics. In: 10th IFAC CAMS; September; Trondheim. IFAC-PapersOnLine 49; 2016. p. 440-445

[18] Piersson WJ, Moskowitz L. A proposed spectral form for fully developed wind seas based on the similarity of S.A. Kitagorodskii. Journal of Geophysical Research. 1964;**96**(2)

[19] ITTC. Report of the Committee on Waves. Final Report and Recommendations to the 23rd International Towing Tank Conference. 2002;505-551

[20] Hasselmann K, Barnet TP, Bouws E, Carlson H, Cartwright DE, Enke K, Ewing JA, Gienapp H, Hasselmann DE, Krusemann P, Meerburg A, Müller P, Olbers DJ, Richter K, Seil W, Walden H. Measurements of wind-wave growth and swell decay during the joint North Sea wave project (JONSWAP). Ergänzungsheft zur Deutschen Hydrographischen Zeitschrift. 1973;**Reihe A(8)**(12):95

[21] Ginsberg JH. Advanced Engineering Dynamics. 2nd ed. New York: Cambridge University Press; 2004

[22] Woernle C. Dynamic of Multi-Body Systems. Rostock: University of Rostock, Lesson script; 2001

[23] Schiehlen W, Eberhard P. Technische Dynamik–Rechnergestützte Modellierung mechanischer Systeme im Maschinen- und Fahrzeugbau. 4th ed. Springer Vieweg; 2014. pp. 24-28. DOI: ISBN 978-3-658-06184-5

[24] Korte H, Ihmels I, Richter J, Zerhusen B, Hahn A. Offshore training simulations. In: 9th IFAC Manoeuvring and Control of Marine Crafts; 19–21 September 2012; Arenzano (IT). IFAC; 2012. pp. 37-42. DOI: ISSN 1474-6670

[25] Blass A, Gurevich Y. Matrix transformation is complete for the average case. SIAM Journal on Computing. 1995;**24**(1):3-29